DESIGN OF SQUARE PATCH MICROSTRIP ANTENNA FOR CIRCULAR POLARIZATION USGIN IE3D SOFTWARE

A THESIS SUBMITTED IN PARTIAL FULFILLMENT OF THE REQUIREMENTS FOR THE DEGREE OF

Bachelor of technology in 'Electronics and Instrumentation'

BY

Amritesh
(10507036)

Kshetrimayum Milan Singh
(10507029)

UNDER THE GUIDANCE OF

Professor S. K. Behera,

ELECTRONICS AND COMMUNICATION ENGINEERING
NATIONAL INSTITUTE OF TECHNOLOGY
ROURKELA, ORISSA,
INDIA

CERTIFICATE

*This is to certify that the thesis entitled "**Design of Square Patch Microstrip Antenna for Circular polarization Using IE3D Software** " by **Mr. Amritesh** and **Mr. Kshetrimayum Milan Singh**, submitted to the National Institute of Technology, Rourkela for the award of Bachelor of Technology in Electronics and Instrumentation Engineering, is a record of bonafide research work carried out by them in the department of Electronics and Communication Engineering, National Institute of Technology, Rourkela under my supervision. I believe that this thesis fulfills part of the requirements for the award of degree of Bachelor of Technology. The results embodied in the thesis have not been submitted for the award of any other degree.*

Prof. S. K. Behera
Department of ECE
National Institute of Technology
Rourkela- 769008

ACKNOWLEDGMENT

We place on record and warmly acknowledge the continuous encouragement, invaluable supervision, timely suggestions and inspired guidance offered by our guide **Dr. S. K. Behera**, Professor, National Institute of Technology, Rourkela, in bringing this report to a successful completion.

We are once again grateful to **Prof G. S. Rath, Prof G. Panda, Prof K. K. Mahapatra, Prof S. Meher, Prof T.K. Dan, Prof S. K. Patra, Prof U.C Pati, Prof D.P Acharya, Prof A. K. Sahoo, Prof P. K. Sahu, and Prof P. Singh** for permitting us to make use of the facilities available in the department to carry out the project successfully. We would like to give sincere thanks to our seniors **Mr. Pendam Chandrashekhar** and **Mr. Yogesh Choukiker** who helped us through the entire duration of the project. Last but not the least we express our sincere thanks to all our friends who have patiently extended all kind of help for accomplishing this undertaking.

Finally we extend our gratitude to one and all who are directly or indirectly involved in the successful completion of this project work.

Amritesh (10507036)

Kshetrimayum Milan Singh(10507029)

Abstract

Communication between humans was first by sound through voice. With the desire for slightly more distance communication came, devices such as drums, then, visual methods such as signal flags and smoke signals were used. These optical communication devices, of course, utilized the light portion of the electromagnetic spectrum. It has been only very recent in human history that the electromagnetic spectrum, outside the visible region, has been employed for communication, through the use of radio. One of humankind's greatest natural resources is the electromagnetic spectrum and the antenna has been instrumental in harnessing this resource.

The thesis provides a detailed study of how to design and fabricate a probe-fed Square Microstrip Patch Antenna using IE3D software and study the effect of antenna dimensions Length (L), and substrate parameters relative Dielectric constant (ε_r), substrate thickness (t) on the Radiation parameters of Bandwidth and Beam-width.

Contents

CHAPTER 1

INTRODUCTION

Communication between humans was first by sound through voice. With the desire for slightly more distance communication came, devices such as drums, then, visual methods such as signal flags and smoke signals were used. These optical communication devices, of course, utilized the light portion of the electromagnetic spectrum. It has been only very recent in human history that the electromagnetic spectrum, outside the visible region, has been employed for communication, through the use of radio. One of humankind's greatest natural resources is the electromagnetic spectrum and the antenna has been instrumental in harnessing this resource.

1.1 Aim and Objectives

Microstrip patch antenna used to send onboard parameters of article to the ground while under operating conditions. The aim of the thesis is to design and fabricate an probe-fed Square Microstrip Patch Antenna and study the effect of antenna dimensions Length (L), and substrate parameters relative Dielectric constant (ε_r), substrate thickness (t) on the Radiation parameters of Bandwidth and Beam-width.

1.2 Overview of Microstrip Antenna

A microstrip antenna consists of conducting patch on a ground plane separated by dielectric substrate. This concept was undeveloped until the revolution in electronic circuit miniaturization and large-scale integration in 1970. After that many authors have described the radiation from the ground plane by a dielectric substrate for different configurations. The early work of Munson on micro strip antennas for use as a low profile

flush mounted antennas on rockets and missiles showed that this was a practical concept for use in many antenna system problems. Various mathematical models were developed for this antenna and its applications were extended to many other fields. The number of papers, articles published in the journals for the last ten years, on these antennas shows the importance gained by them. The micro strip antennas are the present day antenna designer's choice. Low dielectric constant substrates are generally preferred for maximum radiation. The conducting patch can take any shape but rectangular and circular configurations are the most commonly used configuration. Other configurations are complex to analyze and require heavy numerical computations. A microstrip antenna is characterized by its Length, Width, Input impedance, and Gain and radiation patterns. Various parameters of the microstrip antenna and its design considerations were discussed in the subsequent chapters. The length of the antenna is nearly half wavelength in the dielectric; it is a very critical parameter, which governs the resonant frequency of the antenna. There are no hard and fast rules to find the width of the patch.

1.3 Waves on Microstrip

The mechanisms of transmission and radiation in a microstrip can be understood by considering a point current source (Hertz dipole) located on top of the grounded dielectric substrate (fig. 1.1) This source radiates electromagnetic waves. Depending on the direction toward which waves are transmitted, they fall within three distinct categories, each of which exhibits different behaviors.

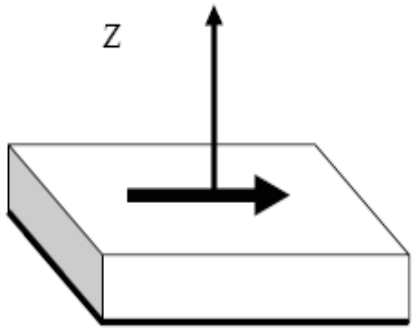

Figure 1.1 Hertz dipole on a microstrip substrate

1.3.1 Surface Waves

The waves transmitted slightly downward, having elevation angles θ between π/2and π - arcsin ($1/\sqrt{\varepsilon_r}$), meet the ground plane, which reflects them, and then meet the dielectric-to-air boundary, which also reflects them (total reflection condition). The magnitude of the field amplitudes builds up for some particular incidence angles that leads to the excitation of a discrete set of surface wave modes; which are similar to the modes in metallic waveguide.

The fields remain mostly trapped within the dielectric, decaying exponentially above the

interface (fig1.2). The vector α, pointing upward, indicates the direction of largest attenuation. The wave propagates horizontally along β, with little absorption in good quality dielectric. With two directions of α and β orthogonal to each other, the wave is a non-uniform plane wave. Surface waves spread out in cylindrical fashion around the excitation point, with field amplitudes decreasing with distance (r), say1/*r*, more slowly than space waves. The same guiding mechanism provides propagation within optical fibers.

Surface waves take up some part of the signal's energy, which does not reach the intended

user. The signal's amplitude is thus reduced, contributing to an apparent attenuation or a decrease in antenna efficiency. Additionally, surface waves also introduce spurious

coupling between different circuit or antenna elements. This effect severely degrades the performance of microstrip filters because the parasitic interaction reduces the isolation in the stop bands.

In large periodic phased arrays, the effect of surface wave coupling becomes particularly

obnoxious, and the array can neither transmit nor receive when it is pointed at some particular directions (blind spots). This is due to a resonance phenomenon, when the surface waves excite in synchronism the Floquet modes of the periodic structure. Surface waves reaching the outer boundaries of an open microstrip structure are reflected and diffracted by the edges. The diffracted waves provide an additional contribution to radiation, degrading the antenna pattern by raising the side lobe and the cross polarization levels. Surface wave effects are mostly negative, for circuits and for antennas, so their excitation should be suppressed if possible.

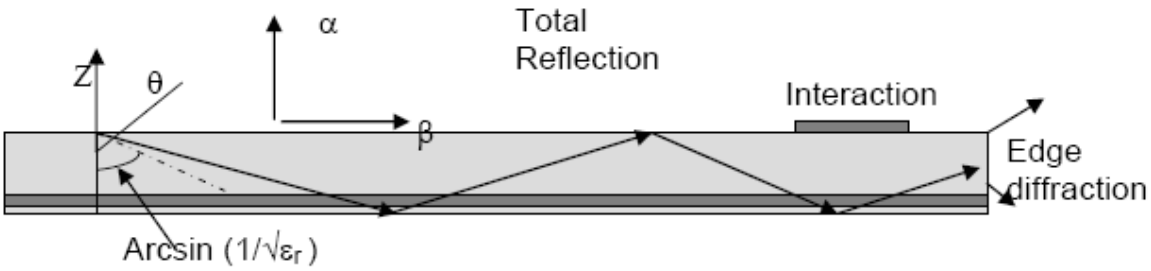

Figure 1.2.Surface waves

1.3.2 Leaky Waves

Waves directed more sharply downward, with θ angles between π - arcsin ($1/\sqrt{\varepsilon_r}$) and π, are also reflected by the ground plane but only partially by the dielectric-to-air boundary. They progressively leak from the substrate into the air (Fig 1.3), hence their name laky waves, and eventually contribute to radiation. The leaky waves are also non-uniform plane waves for which the attenuation direction α points downward, which may appear to be rather odd; the amplitude of the waves increases as one moves away from the dielectric surface. This apparent paradox is easily understood by looking at the figure 1.3; actually, the field amplitude increases as one move away from the substrate because the wave radiates from a point where the signal amplitude is larger. Since the structure is

finite, this apparent divergent behavior can only exist locally, and the wave vanishes abruptly as one crosses the trajectory of the first ray in the figure.

In more complex structures made with several layers of different dielectrics, leaky waves can be used to increase the apparent antenna size and thus provide a larger gain. This occurs for favorable stacking arrangements and at a particular frequency. Conversely, leaky waves are not excited in some other multilayer structures.

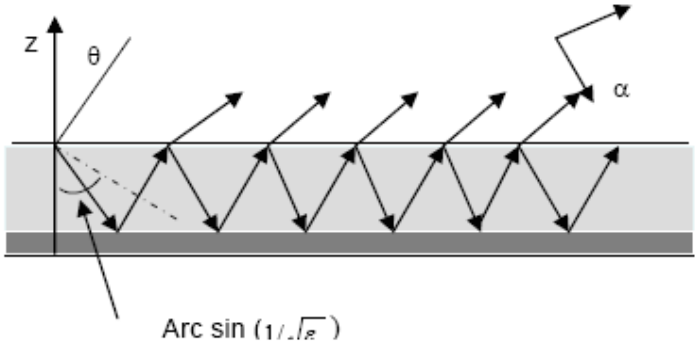

Figure 1.3 Leaky waves

1.3.3 Guided Waves

When realizing printed circuits, one locally adds a metal layer on top of the substrate, which modifies the geometry, introducing an additional reflecting boundary. Waves directed into the dielectric located under the upper conductor bounce back and forth on the metal boundaries, which form a parallel plate waveguide. The waves in the metallic guide can only exist for some Particular values of the angle of incidence, forming a discrete set of waveguide modes. The guided waves provide the normal operation of all transmission lines and circuits, in which the electromagnetic fields are mostly concentrated in the volume below the upper conductor. On the other hand, this buildup of electromagnetic energy is not favorable for patch antennas, which behave like resonators with a limited frequency bandwidth.

1.4 Antenna Characteristics

An antenna is a device that is made to efficiently radiate and receive radiated electromagnetic waves. There are several important antenna characteristics that should be considered when choosing an antenna for your application as follows:

- Antenna radiation patterns
- Power Gain
- Directivity
- Polarization

1.5 Organization of the Thesis

An introduction to microstrip antennas was given in Chapter 2. Apart from the advantages and disadvantages, the various feeding techniques and models of analysis were listed.

Chapter 3 deals with different types of patches and feeding techniques for circular polarization. The technique of dual feed is also discussed. Various types of power divider circuits that have been successfully employed in a feed network of a CP patch are also discussed.

Chapter 4 provides the design and development of microstrip antenna. It provides information about IE3d Software for simulation of Microstrip Antennas, which will be used for cross verification of results for designed antennas. Chapter 5 includes conclusions and future scope to this project work.

CHAPTER 2

MICROSTRIP PATCH ANTENNA

Microstrip antennas are attractive due to their light weight, conformability and low cost. These antennas can be integrated with printed strip-line feed networks and active devices. This is a relatively new area of antenna engineering. The radiation properties of micro strip structures have been known since the mid 1950's.

The application of this type of antennas started in early 1970's when conformal antennas were required for missiles. Rectangular and circular micro strip resonant patches have been used extensively in a variety of array configurations. A major contributing factor for recent advances of microstrip antennas is the current revolution in electronic circuit miniaturization brought about by developments in large scale integration. As conventional antennas are often bulky and costly part of an electronic system, micro strip antennas based on photolithographic technology are seen as an engineering breakthrough.

2.1 Introduction

In its most fundamental form, a Microstrip Patch antenna consists of a radiating patch on one side of a dielectric substrate which has a ground plane on the other side as shown in Figure 2.1. The patch is generally made of conducting material such as copper or gold and can take any possible shape. The radiating patch and the feed lines are usually photo etched on the dielectric substrate.

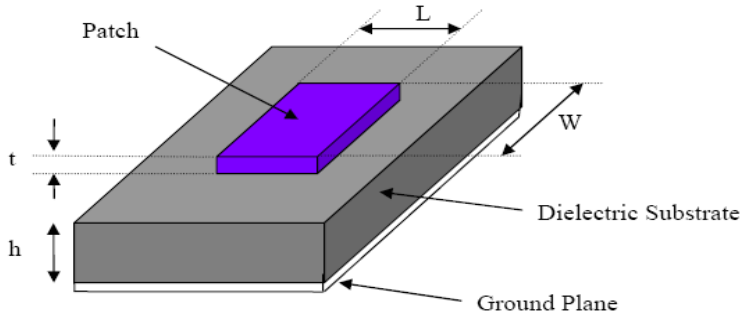

Figure 2.1 Structure of a Microstrip Patch Antenna

In order to simplify analysis and performance prediction, the patch is generally square, rectangular, circular, triangular, and elliptical or some other common shape as shown in Figure 2.2. For a rectangular patch, the length L of the patch is usually $0.3333\lambda_o < L < 0.5\ \lambda_o$, where λ_o is the free-space wavelength. The patch is selected to be very thin such that $t << \lambda_o$ (where t is the patch thickness). The height h of the dielectric substrate is usually $0.003\ \lambda_o \leq h \leq 0.05\ \lambda_o$. The dielectric constant of the substrate (ε_r) is typically in the range $2.2 \leq \varepsilon_r \leq 12$.

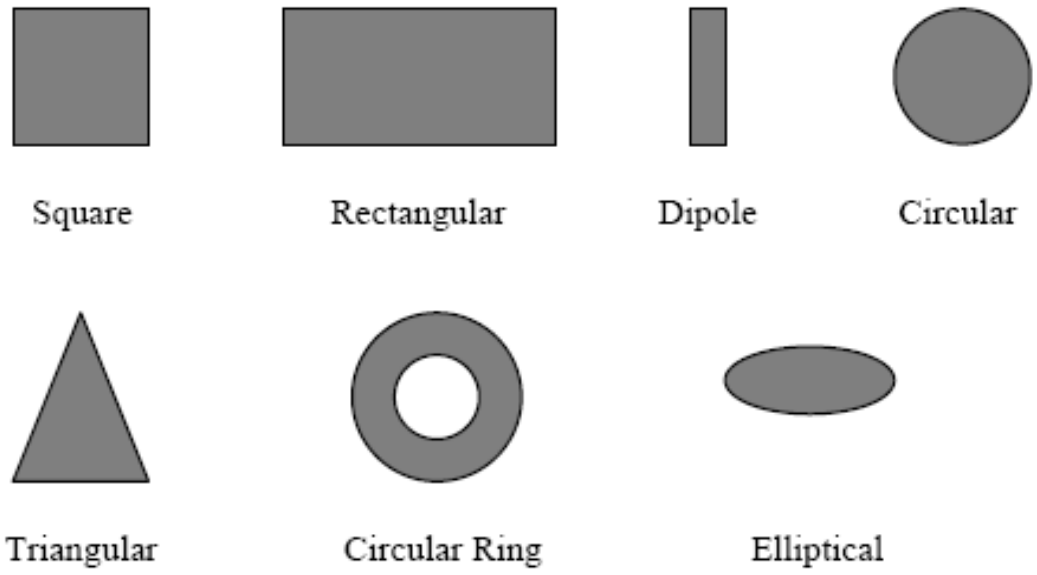

Figure2.2 Common Shapes of microstrip patch elements

Microstrip patch antennas radiate primarily because of the fringing fields between the patch edge and the ground plane. For good antenna performance, a thick dielectric substrate having a low dielectric constant is desirable since this provides better efficiency, larger bandwidth and better radiation. However, such a configuration leads to a larger antenna size. In order to design a compact Microstrip patch antenna, substrates with higher dielectric constants must be used which are less efficient and result in narrower bandwidth. Hence a trade-off must be realized between the antenna dimensions and antenna performance.

2.2 Advantages and Disadvantages

Microstrip patch antennas are increasing in popularity for use in wireless applications due to their low-profile structure. Therefore they are extremely compatible for embedded antennas in handheld wireless devices such as cellular phones, pagers etc... The telemetry and communication antennas on missiles need to be thin and conformal and are often in the form of Microstrip patch antennas. Another area where they have been used successfully is in Satellite communication. Some of their principal advantages discussed by Kumar and Ray are given below:

- Light weight and low volume.
- Low profile planar configuration which can be easily made conformal to host surface.
- Low fabrication cost, hence can be manufactured in large quantities.
- Supports both, linear as well as circular polarization.
- Can be easily integrated with microwave integrated circuits (MICs).
- Capable of dual and triple frequency operations.
- Mechanically robust when mounted on rigid surfaces.

Microstrip patch antennas suffer from more drawbacks as compared to conventional

antennas. Some of their major disadvantages discussed by and Garg et al are given below:

- Narrow bandwidth.
- Low efficiency.
- Low Gain.
- Extraneous radiation from feeds and junctions.
- Poor end fire radiator except tapered slot antennas.
- Low power handling capacity.
- Surface wave excitation.

Microstrip patch antennas have a very high antenna quality factor (Q). It represents the losses associated with the antenna where a large Q leads to narrow bandwidth and low efficiency. Q can be reduced by increasing the thickness of the dielectric substrate. But as the thickness increases, an increasing fraction of the total power delivered by the source goes into a surface wave. This surface wave contribution can be counted as an unwanted power loss since it is ultimately scattered at the dielectric bends and causes degradation of the antenna characteristics. Other problems such as lower gain and lower power handling capacity can be overcome by using an array configuration for the elements.

2.3 Feed Techniques

Microstrip patch antennas can be fed by a variety of methods. These methods can be classified into two categories- contacting and non-contacting. In the contacting method, the RF power is fed directly to the radiating patch using a connecting element such as a microstrip line. In the non-contacting scheme, electromagnetic field coupling is done to transfer power between the microstrip line and the radiating patch. The four most popular feed techniques used are the microstrip line, coaxial probe (both contacting schemes), aperture coupling and proximity coupling (both non-contacting schemes).

2.3.1 Microstrip Line Feed

In this type of feed technique, a conducting strip is connected directly to the edge of the Microstrip patch as shown in Figure 2.3. The conducting strip is smaller in width as compared to the patch and this kind of feed arrangement has the advantage that the feed can be etched on the same substrate to provide a planar structure.

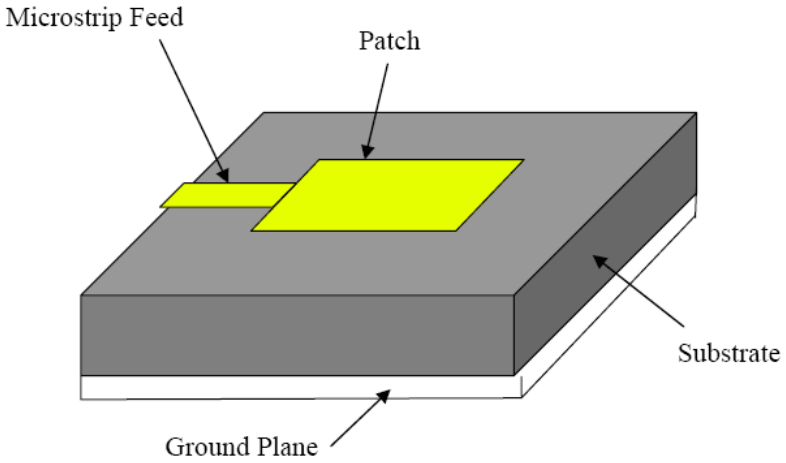

Figure 2.3 Microstrip Line Feed

The purpose of the inset cut in the patch is to match the impedance of the feed line to the patch without the need for any additional matching element. This is achieved by properly controlling the inset position. Hence this is an easy feeding scheme, since it provides ease of fabrication and simplicity in modeling as well as impedance matching. However as the thickness of the dielectric substrate being used, increases, surface waves and spurious feed radiation also increases, which hampers the bandwidth of the antenna. The feed radiation also leads to undesired cross polarized radiation.

2.3.2 Coaxial Feed

The Coaxial feed or probe feed is a very common technique used for feeding Microstrip patch antennas. As seen from Figure 2.4, the inner conductor of the coaxial connector extends through the dielectric and is soldered to the radiating patch, while the outer conductor is connected to the ground plane.

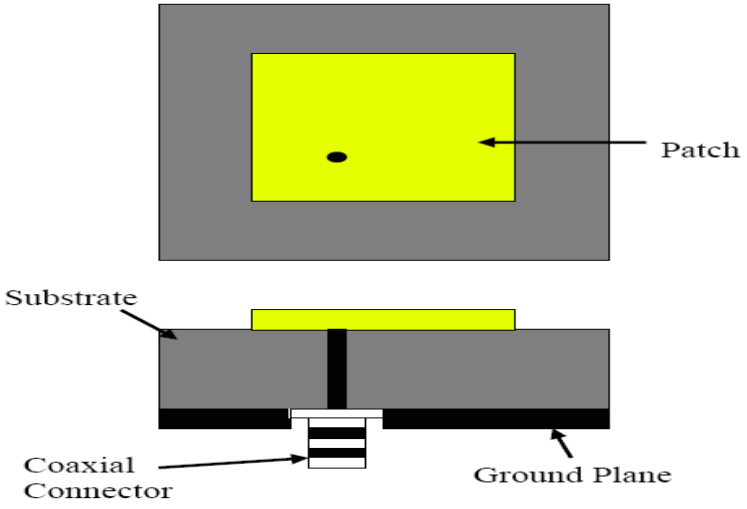

Figure 2.4 Probe fed Rectangular Microstrip Patch Antenna

The main advantage of this type of feeding scheme is that the feed can be placed at any desired location inside the patch in order to match with its input impedance. This feed method is easy to fabricate and has low spurious radiation. However, a major disadvantage is that it provides narrow bandwidth and is difficult to model since a hole has to be drilled in the substrate and the connector protrudes outside the ground plane, thus not making it completely planar for thick substrates ($h > 0.02\lambda_o$). Also, for thicker substrates, the increased probe length makes the input impedance more inductive, leading to matching problems. It is seen above that for a thick dielectric substrate, which provides broad bandwidth, the microstrip line feed and the coaxial feed suffer from numerous disadvantages. The non-contacting feed techniques which have been discussed below, solve these issues.

2.3.3 Aperture Coupled Feed

In this type of feed technique, the radiating patch and the microstrip feed line are separated by the ground plane as shown in Figure 2.5. Coupling between the patch and the feed line is made through a slot or an aperture in the ground plane.

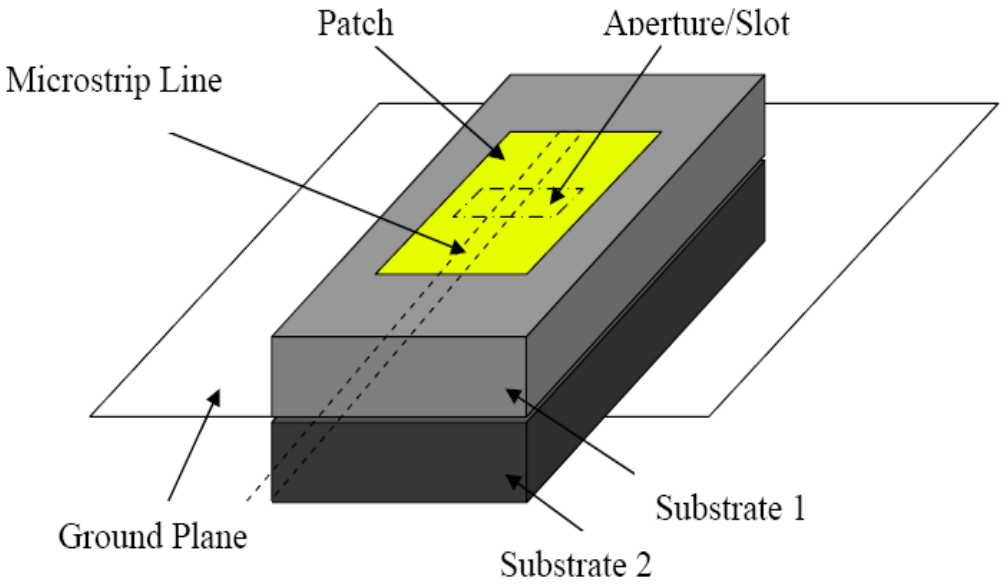

Figure 2.5 Aperture-coupled feed

The coupling aperture is usually centered under the patch, leading to lower cross-polarization due to symmetry of the configuration. The amount of coupling from the feed line to the patch is determined by the shape, size and location of the aperture. Since the ground plane separates the patch and the feed line, spurious radiation is minimized. Generally, a high dielectric material is used for bottom substrate and a thick, low dielectric constant material is used for the top substrate to optimize radiation from the patch. The major disadvantage of this feed technique is that it is difficult to fabricate due to multiple layers, which also increases the antenna thickness. This feeding scheme also provides narrow bandwidth.

2.3.4 Proximity Coupled Feed

This type of feed technique is also called as the electromagnetic coupling scheme. As shown in Figure 2.6, two dielectric substrates are used such that the feed line is between the two substrates and the radiating patch is on top of the upper substrate. The main advantage of this feed technique is that it eliminates spurious feed radiation and provides very high bandwidth (as high as 13%), due to overall increase in the thickness of the microstrip patch antenna. This scheme also provides choices between two different dielectric media, one for the patch and one for the feed line to optimize the individual performances.

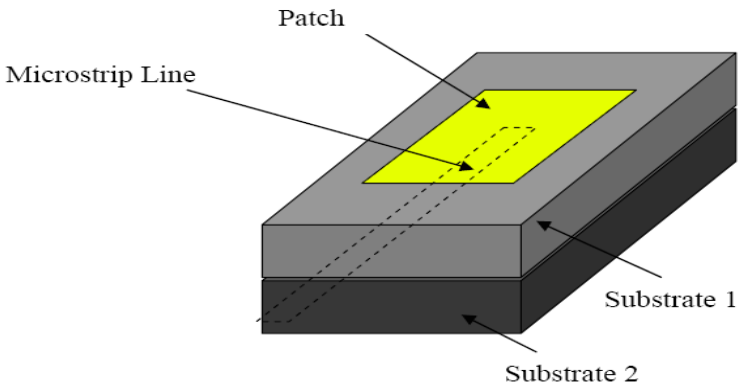

Figure 2.6 Proximity-coupled Feed

Matching can be achieved by controlling the length of the feed line and the width-to-line ratio of the patch. The major disadvantage of this feed scheme is that it is difficult to fabricate because of the two dielectric layers which need proper alignment. Also, there is an increase in the overall thickness of the antenna.

2.4 Methods of Analysis

The preferred models for the analysis of Microstrip patch antennas are the transmission line model, cavity model, and full wave model (which include primarily integral equations/Moment Method). The transmission line model is the simplest of all and it gives good physical insight but it is less accurate. The cavity model is more accurate and gives good physical insight but is complex in nature. The full wave models are extremely accurate, versatile and can treat single elements, finite and infinite arrays, stacked elements, arbitrary shaped elements and coupling. These give less insight as compared to the two models mentioned above and are far more complex in nature.

2.4.1 Transmission Line Model

This model represents the microstrip antenna by two slots of width *W* and height *h*, separated by a transmission line of length L. The microstrip is essentially a non-homogeneous line of two dielectrics, typically the substrate and air.

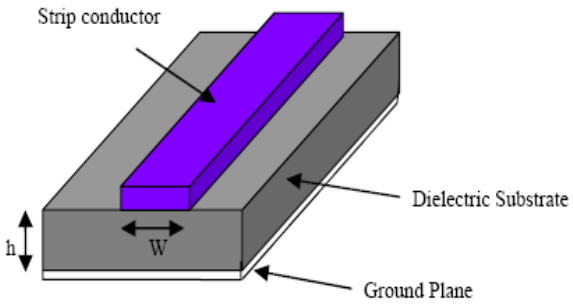

Figure 2.7 Microstrip Line

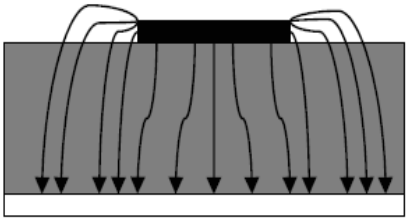

Figure 2.8 Electric Field Lines

Hence, as seen from Figure 2.8, most of the electric field lines reside in the substrate and parts of some lines in air. As a result, this transmission line cannot support pure transverse-electric-magnetic (TEM) mode of transmission, since the phase velocities would be different in the air and the substrate. Instead, the dominant mode of propagation would be the quasi-TEM mode. Hence, an effective dielectric constant (ε_{reff}) must be obtained in order to account for the fringing and the wave propagation in the line. The value of ε_{reff} is slightly less then ε_r because the fringing fields around the periphery of the patch are not confined in the dielectric substrate but are also spread in the air as shown in Figure 3.8 above. The expression for ε_{reff} is given by Balanis as:

$$\varepsilon_{reff} = \frac{\varepsilon_r + 1}{2} + \frac{\varepsilon_r - 1}{2}\left[1 + 12\frac{h}{W}\right]^{-\frac{1}{2}}$$

Where ε_{reff} = Effective dielectric constant

ε_r = Dielectric constant of substrate

h = Height of dielectric substrate

W = Width of the patch

Consider Figure 2.9 below, which shows a rectangular microstrip patch antenna of length L, width W resting on a substrate of height h. The co-ordinate axis is selected such that the ĺength is along the x direction, width is along the y direction and the height is along the z direction.

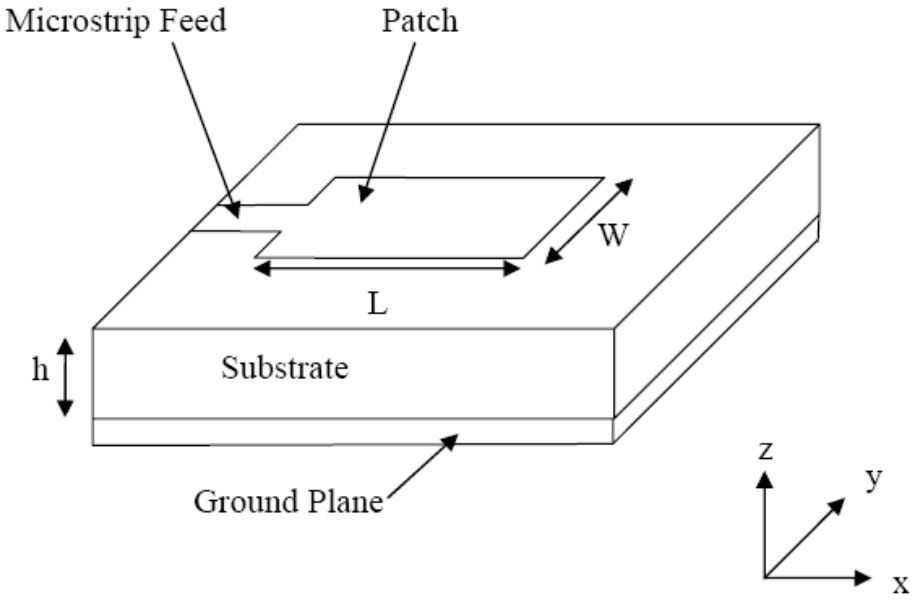

Figure 2.9 Microstrip Patch Antennas

In order to operate in the fundamental TM_{10} mode, the length of the patch must be slightly less than λ/2 where λ is the wavelength in the dielectric medium and is equal to $\lambda_o/\sqrt{\varepsilon reff}$ where λ_o is the free space wavelength. The TM_{10} mode implies that the field varies one λ/2 cycle along the length, and there is no variation along the width of the patch. In the Figure 2.10 shown below, the microstrip patch antenna is represented by two slots, separated by a transmission line of length L and open circuited at both the ends. Along the width of the patch, the voltage is maximum and current is minimum due to the open ends. The fields at the edges can be resolved into normal and tangential components with respect to the ground plane.

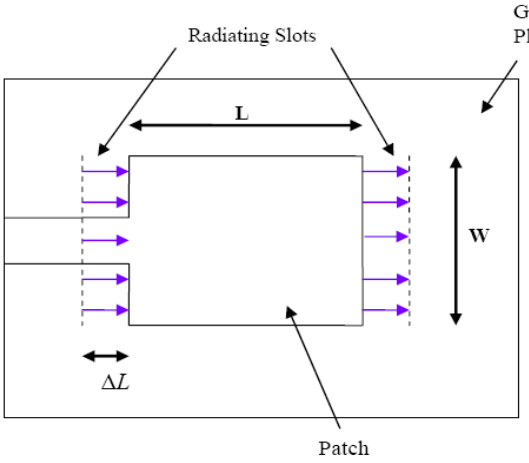

Figure 2.10 Top View of Antenna

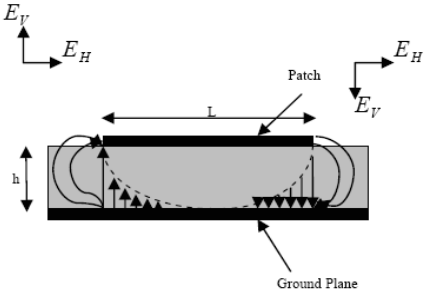

Figure 2.11 Side View of Antenna

It is seen from Figure 2.11 that the normal components of the electric field at the two edges along the width are in opposite directions and thus out of phase since the patch is λ/2 long and hence they cancel each other in the broadside direction. The tangential components (seen in Figure 2.11), which are in phase, means that the resulting fields combine to give maximum radiated field normal to the surface of the structure. Hence the edges along the width can be represented as two radiating slots, which are λ/2 apart and excited in phase and radiating in the half space above the ground plane. The fringing fields along the width can be modeled as radiating slots and electrically the patch of the microstrip antenna looks greater than its physical dimensions. The dimensions of the patch along its length have now been extended on each end by a distance ΔL, which is given empirically by Hammerstad as:

$$\Delta L = 0.412h\frac{\left(\varepsilon_{reff}+0.3\right)\left(\frac{W}{h}+0.264\right)}{\left(\varepsilon_{reff}-0.258\right)\left(\frac{W}{h}+0.8\right)}$$

The effective length of the patch L_{eff} now becomes:

$$L_{eff} = L + 2\Delta L$$

For a given resonance frequency f_o, the effective length is given by [9] as:

$$L_{eff} = \frac{c}{2f_o\sqrt{\varepsilon_{reff}}}$$

For a rectangular Microstrip patch antenna, the resonance frequency for any TM_{mn} mode is given by James and Hall as:

$$f_o = \frac{c}{2\sqrt{\varepsilon_{reff}}}\left[\left(\frac{m}{L}\right)^2+\left(\frac{n}{W}\right)^2\right]^{\frac{1}{2}}$$

Where m and n are modes along L and W respectively.

For efficient radiation, the width W is given by Bahl and Bhartia [15] as:

$$W = \frac{c}{2f_o\sqrt{\frac{(\varepsilon_r+1)}{2}}}$$

2.4.2 Cavity Model

Although the transmission line model discussed in the previous section is easy to use, it has some inherent disadvantages. Specifically, it is useful for patches of rectangular design and it ignores field variations along the radiating edges. These disadvantages can be overcome by using the cavity model. A brief overview of this model is given below.

In this model, the interior region of the dielectric substrate is modeled as a cavity bounded by electric walls on the top and bottom. The basis for this assumption is the following observations for thin substrates ($h << \lambda$).

- Since the substrate is thin, the fields in the interior region do not vary much in the z direction, i.e. normal to the patch.
- The electric field is z directed only, and the magnetic field has only the transverse components H_x and H_y in the region bounded by the patch metallization and the ground plane. This observation provides for the electric walls at the top and the bottom.

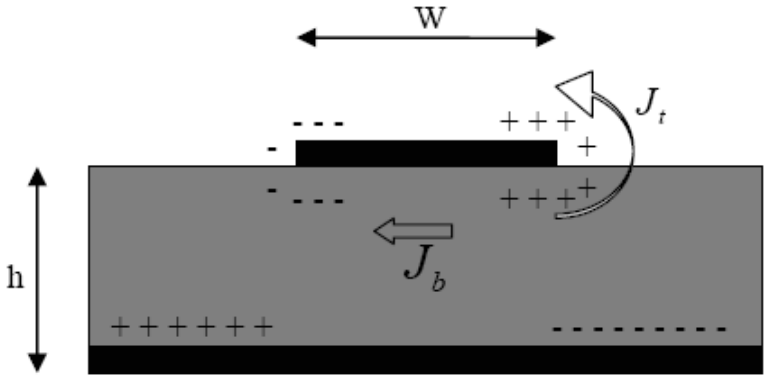

Figure 2.12 Charge distribution and current density creation on the microstrip patch

Consider Figure 2.12 shown above. When the microstrip patch is provided power, a charge distribution is seen on the upper and lower surfaces of the patch and at the bottom of the ground plane. This charge distribution is controlled by two mechanisms-an

attractive mechanism and a repulsive mechanism as discussed by Richards. The attractive mechanism is between the opposite charges on the bottom side of the patch and the ground plane, which helps in keeping the charge concentration intact at the bottom of the patch. The repulsive mechanism is between the like charges on the bottom surface of the patch, which causes pushing of some charges from the bottom, to the top of the patch. As a result of this charge movement, currents flow at the top and bottom surface of the patch. The cavity model assumes that the height to width ratio (i.e. height of substrate and width of the patch) is very small and as a result of this the attractive mechanism dominates and causes most of the charge concentration and the current to be below the patch surface. Much less current would flow on the top surface of the patch and as the height to width ratio further decreases, the current on the top surface of the patch would be almost equal to zero, which would not allow the creation of any tangential magnetic field components to the patch edges. Hence, the four sidewalls could be modeled as perfectly magnetic conducting surfaces. This implies that the magnetic fields and the electric field distribution beneath the patch would not be disturbed. However, in practice, a finite width to height ratio would be there and this would not make the tangential magnetic fields to be completely zero, but they being very small, the side walls could be approximated to be perfectly magnetic conducting.

Since the walls of the cavity, as well as the material within it are lossless, the cavity would not radiate and its input impedance would be purely reactive. Hence, in order to account for radiation and a loss mechanism, one must introduce a radiation resistance R_R and a loss resistance R_L. A lossy cavity would now represent an antenna and the loss is taken into account by the effective loss tangent δ_{eff} which is given as:

$$\delta_{eff} = 1/Q_T$$

Q_T is the total antenna quality factor and has been expressed by [4] in the form:

$$\frac{1}{Q_T} = \frac{1}{Q_d} + \frac{1}{Q_c} + \frac{1}{Q_r}$$

- Q_d represents the quality factor of the dielectric and is given as :

$$Q_d = \frac{\omega_r W_T}{P_d} = \frac{1}{\tan\delta}$$

where ω_r is the angular resonant frequency.

W_T is the total energy stored in the patch at resonance.

P_d is the dielectric loss.

$\tan\delta$ is the loss tangent of the dielectric.

- Q_c represents the quality factor of the conductor and is given as :

$$Q_c = \frac{\omega_r W_T}{P_c} = \frac{h}{\Delta}$$

where P_c is the conductor loss.

Δ is the skin depth of the conductor.

h is the height of the substrate.

- Q_r represents the quality factor for radiation and is given as:

$$Q_r = \frac{\omega_r W_T}{P_r}$$

where P_r is the power radiated from the patch.

Substituting equations (3.8), (3.9), (3.10) and (3.11) in equation (3.7), we get

$$\delta_{eff} = \tan\delta + \frac{\Delta}{h} + \frac{P_r}{\omega_r W_T}$$

Thus, the above equation describes the total effective loss tangent for the microstrip patch antenna.

Chapter 3
Circularly Polarized Microstrip Antennas

3.1 Introduction

In this chapter, the design consideration for circularly polarized microstrip antennas is presented. Various techniques for circularly polarized radiation generation and bandwidth enhancement are also discussed.

3.2 Different Types of Circularly Polarized Antennas.

Generally antenna radiates an elliptical polarization, which is defined by three parameters: axial ratio, tilt angle and sense of rotation. When the axial ratio is infinite or zero, the polarization becomes linear with the tilt angle defining the orientation. The quality of linear polarization is usually indicated by the level of the cross polarization. For the unity axial ratio, a perfect circular polarization results and the tilt angle is not applicable. In general the axial ratio is used to specify the quality of circularly polarized waves.

Antennas produce circularly polarized waves when two orthogonal field components with equal amplitude but in phase quadrature are radiated. Various antennas are capable of satisfying these requirements. They can be classified as a resonator and traveling-wave types. A resonator-type antenna consists of a single patch antenna that is capable of simultaneously supporting two orthogonal modes in phase quadrature or an array of linearly polarized resonating patches with proper orientation and phasing. A traveling-wave type of antenna is usually constructed from a microstrip transmission line. It generates circular polarization by radiating orthogonal components with appropriate phasing along discontinuities is the travelling-wave line.

3.2.1 Microstrip Patch Antennas

A microstrip antenna is a resonator type antenna. It is usually designed for single mode operation that radiates mainly linear polarization. For a circular polarization radiation, a patch must support orthogonal fields of equal magnitude but in-phase quadrature. This requirement can be accomplished by single patch with proper excitations or by an array of patches with an appropriate arrangement and phasing.

Circularly Polarized Patch

A microstrip patch is one of the most widely used radiators for circular polarization. Figure 3.1shows some patches, including square, circular, pentagonal, equilateral triangular, ring, and elliptical shapes which are capable of circular polarization operation. However square and circular patches are widely utilized in practice.

A single patch antenna can be made to radiate circular polarization if two orthogonal patch modes are simultaneously excited with equal amplitude and $\pm 90^{\circ}$ out of phase with sign determining the sense of rotation. Two types of feeding schemes can accomplish the task as given in figure 3.2. The first type is a dual-orthogonal feed, which employs an external power divider network. The other is a single point for which an external power divider is not required.

Dual-Orthogonal Fed circularly Polarized Patch

The fundamental configurations of a dual-orthogonal fed circularly polarized patch using an external power divider is shown in figure 3.3. The patch is usually square or circular. The dual-orthogonal feeds excite two orthogonal modes with equal amplitude but in-phase quadrature. Several power divider circuits that have been successfully employed for CP generation include the quadrature hybrid, the ring hybrid, the Wilkinson power divider, and the T-junction power splitter. The quadrature hybrid splits the input into two outputs with equal magnitude but 90^0 out of phase. Other types of dividers, however, need a quarter-wavelength line in one of the output arms to produce a 90^0 phase shift at the two feeds. Consequently, the quadrature hybrid provides a broader axial ratio bandwidth. These splitters can be easily constructed from various planar transmission lines.

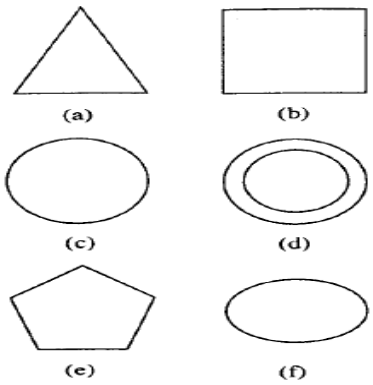

Figure 3.1 Various types of circularly polarized microstrip patch antennas: (a) triangular patch, (b) square patch, (c) circular patch, (d) ring, (e) pentagonal patch, and (f) elliptical patch.

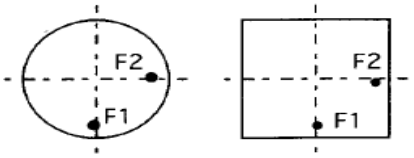

(a)

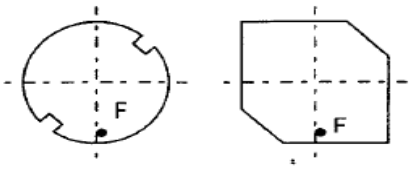

(b)

Figure 3.2 Two types of excitations for circularly polarized microstrip antennas: (a) dual-fed patch and (b) singly fed patch.

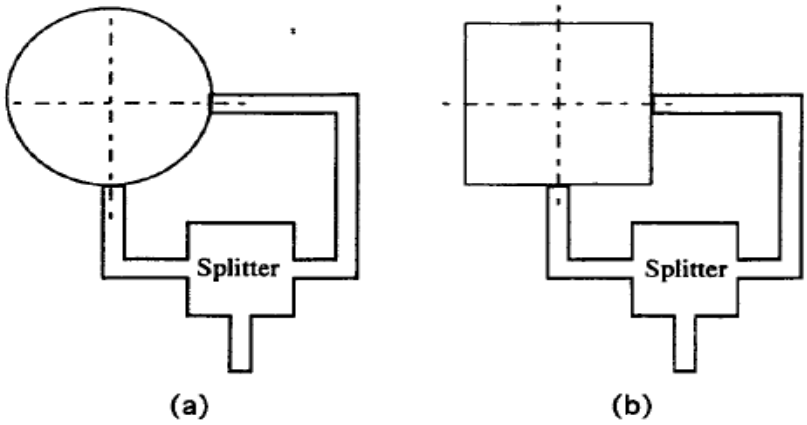

Figure 3.3 Typical configurations of dual-fed circularly Polarized microstrip antennas:

(a)circular patch and (b) square patch

Singly Fed Circularly Polarized Patch

Typical configurations for a singly fed CP microstrip antennas are shown in figure 3.4 A single point feed patch capable of producing CP radiation is very desirable is situations where it is difficult to accommodate dual-orthogonal feeds with a power divider network.

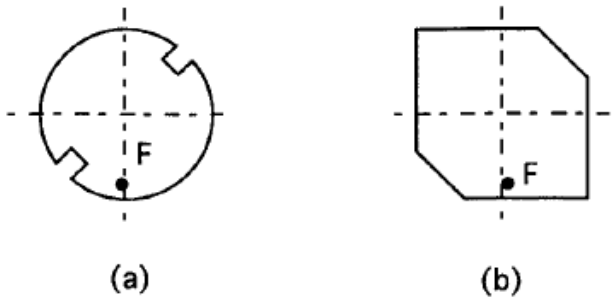

Figure 3.4 Typical configurations of singly fed circularly polarized microstrip antennas:

(a)Circular patch and (b) square patch

Because a patch with single-point feed generally radiates linear polarization, in order to radiate CP, it is necessary for two orthogonal patch modes with equal amplitude an in-

phase quadrature to be induced. This can be accomplished by slightly perturbing a patch at appropriate locations with respect to the feed.

Purturbation configurations for generating CP operate on the principle of detuning degenrate modes of a symmetrical patch by perturabation segments as shown in figure 3.5. The fields of a singly fed patch can be resolved into two orthogonal degenerates modes 1 and 2. Proper purturbation segments will detune the frequency response of mode 2 such that, at the operating frequency f_0, the axial ratio rapidly degrades while the input match remains acceptable. The actual detunig occurs either for one or both modes depending on the placement of perturbation segments.

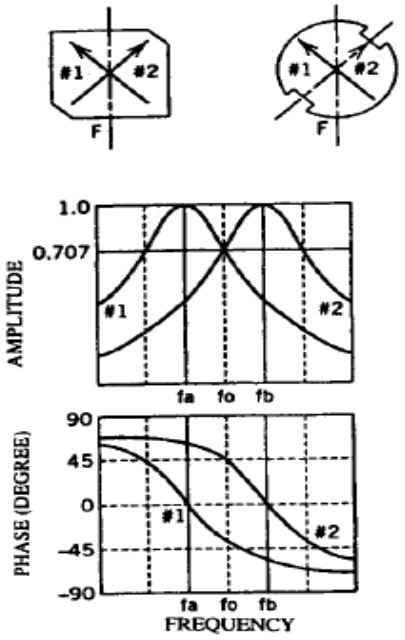

Figure 3.5 Amplitude and phase of orthogonal modes for singly fed circularly polarized mocrostrip antennas.

A circular polarization can also be obtained from a single-point-fed square or circular patch on a normally biased ferrite substrate, as shown in figure 3.6. Pozar demostrated that a singly fed patch radiates both left hand circularly polarized (LHCP) and right hand circularly polarized(RHCP) at the same level and polarity of bias magnetic field; however LHCP and RHCP have different resonan frequencies. At the same operating frequency, the sence of polarization can be reversed by reversing the polarity of

bias field. The axial ratio bandwidth is found to be larger than the impedance bandwidth. The radiation efficiency is on the order of 70%.

Dual circular polarization have also been achieved using a singly fed triangular or pentagonal microstrip antenna. A schematic diagram of an isoceles triangular patch and its feed loci is shown in figure 3.7. A triangular patch radiates CP at dual frequencies, f_1 and f_2, with the separation ratio depending on the aspect ratio b/a. As shown in figure 3.7 RHCP can be changed to LHCP at each frequency by moving the feed location $\acute{\Gamma}_1$to $\acute{\Gamma}_2$ or from $\acute{\Gamma}_4$ to $\acute{\Gamma}_3$. The aspect ratio b/a is generally very close to unity; hence, a triangular patch is almost equilateral. A pentagonal patch in figure 3.8, with the aspect ratio c/a as a design parameter, also behaves in a similar manner. It radiates RHCP when the feed point is on $\acute{\Gamma}_2$ or $\acute{\Gamma}_3$ and LHCP for the feed on $\acute{\Gamma}_1$ to $\acute{\Gamma}_4$.

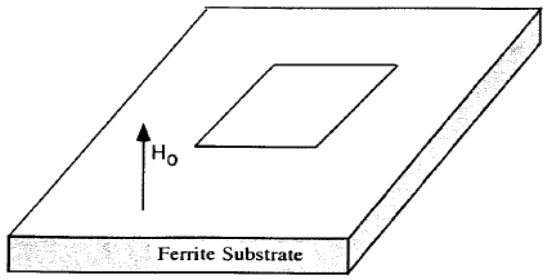

Figure 3.6 Geometry of a ractangular patch antenna on a normally biased ferrite substrate.

Arrays of Linearly Polarized Patches for Circularly Polarized Radiation

Two linear LP patch antennas can be orthogonally arranged as shown in figure 3.9 with one of the patches being fed 90^0 out of phase. The disadvantage of this configuration are

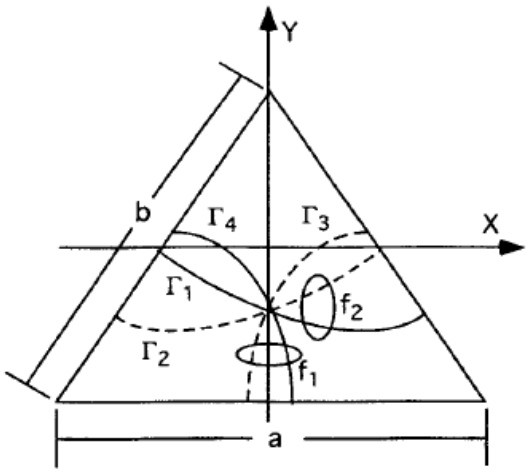

Figure 3.7 Schematic diagram of an isosceles triangular patch and the feed loci for circular polarization radiations: $\acute{\Gamma}_1$ and $\acute{\Gamma}_4$ for RHCP; $\acute{\Gamma}_2$ and $\acute{\Gamma}_3$ for LHCP.

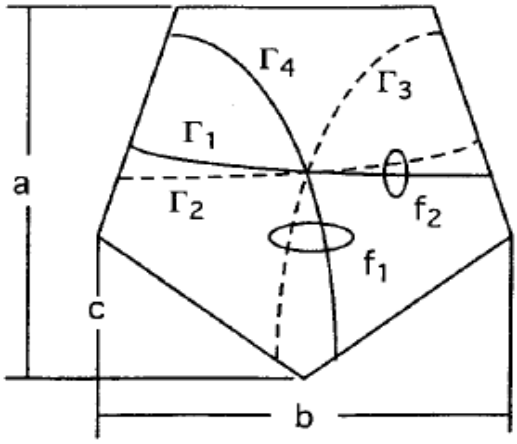

Figure 3.8 Schematic diagram of a pentagonal microstrip patch and the feed loci for circular polarization radiations: $\acute{\Gamma}_1$ and $\acute{\Gamma}_4$ for LHCP; $\acute{\Gamma}_2$ and $\acute{\Gamma}_3$ for RHCP.

larger space requuirements and rapid degradation of CP with angle off the boreisght as a result of spatial phase delay due to different path lenghts from the phase centers of the two radiating elements. An alternative arrangement in figure 3.10 by Huang significantly improves the CP quality. The axial ratio bandwidth of the array substantially increases. The cross-polar are significantly suppressed on the two principle planes, the x-z and the y-z planes, but this is not true on the two diagonal planes.

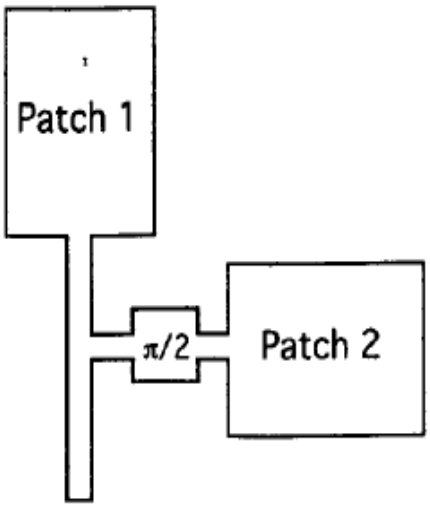

Figure 3.9 Possible arrangement of two linearly polarized patches for circular polarization radiation

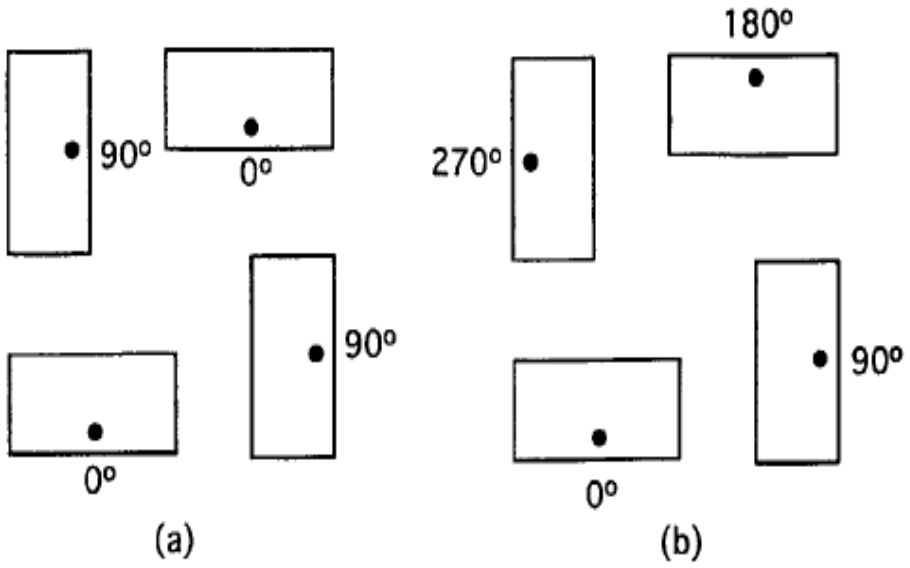

Figure 3.10 2x2 microstrip arrays with LP elements for CP generation: (a) narrow-band arrangement and (b) wide-band arrangement.

3.2.2 Other Types of Circularly Polarized Antennas

Other types of CP antennas are compact in their feed requirements and radiating element configurations. These types are CP antennas, which can be easily constructed from microstrip lines, are described next.

Microstrip Spiral Antennas

To obtain a wide bandwidth, the concept of conventioanl spiral antennas has been applied to microstrip spiral design. A conventional spural radiates good CP because small residual current remains after the active zone, which corresponds to a spiral arm with a wavelength circumference. However, Wood found that this was not true for the case of microstrip spirals. The decaying of a current in microstrip spirals in the active region was not large enough to prevent significant interference radiation from successive turns in the spiral that adversely affected CP performance. Hence, Wood's design took on the form of a sector of a circular transmission line and one turn of a loosely wound spiral with a feed at one end and a matched termination at the other as shown in figure 3.11. The antennas achieve the bandwidth of 40% with axial ratio of less than 3 dB at the cost of reducing the average radiation efficiency to 50 %. Wang and tripp experimented with microstip spirals using microwave absorbing material placed half inside the truncated spiral and half outside to dissipate the residual energy.They were able to achive a bandwidth of 6:1 for patterns.

Array of Composite Elements

A circular polarization can be produced from an array of composite electric and magnetic radiation elements that radiate mutually orthogonal fields with 90˚ phase difference.One such array consists of standing-wave fed slots and strip dipoles as shown in figure 3.12. It is composed of strips on a thin substrate, slots in the ground plane, and a microstrip feed linetarminating in a short circuit. The strip and the slots are a half-wavelength long and are spaced at a quarter-guide wavelenth apart along feed line to provide the 90˚ phase difference requirement. When the strips and the slot are located at

the maximum points of voltage and current standing waves, the array can efficiently produce CP in the broadside direction.

Traveling-Wave Arrays

Altarnating design of CP printed antennas is in te form of a linear of a linear traveling-wave array consisting of microstrip transmission line excitation of microstrip Cp radiating elements. The residual power at the end of the microstrip feed line is dissipated in a termination to prevent reflection that otherwise can adversely degrade CP quality. The element spacing is generally greater then $\lambda_0/2$; thus ,it is possible to use previously described resonator-type CP elements in the design. However,CP radiating elements can also be constructed from orthogonal arrangement of linearly polarizd (LP) radiators as depicted in Figure 3.13, which shows traveling-wave printed dipole and slot arrays.

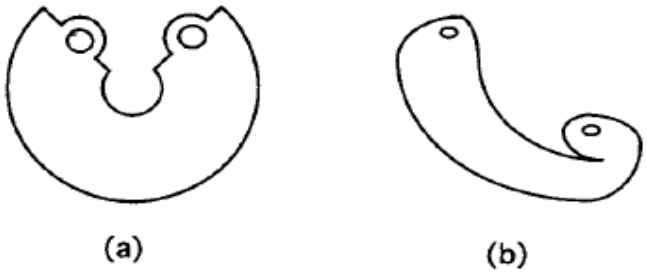

Figure 3.11 Circular polarized curved microstrip line antennas: (a) sector of circular microstrip transmission line and (b) spiral microstrip line antenna.

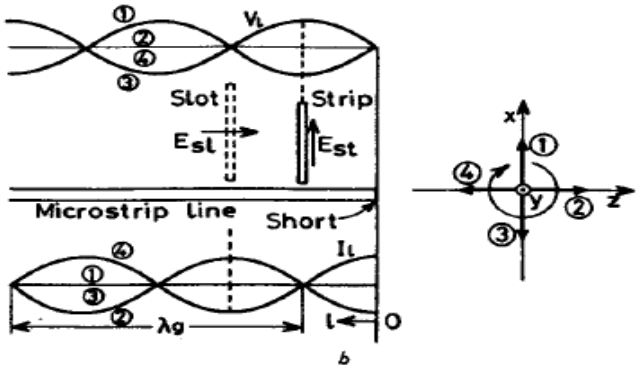

Figure 3.12 Array of composite elements for circular polarization.

In the dipole array , each unit cell consists of inclined half-wavelength printed dipoles arranged along both sides of a microstrip feed line.The spacing D_s between adjacent dipoles in each unit cell is a quarter-guide wavelenght. The spacing D_p between unit cell and the inclined angle α are determined from the desired main beam direction. Slot array arangements can be determined in a similas manner. However, the operation of the slot array requires a reflector under the substrate for back radiation suppression.

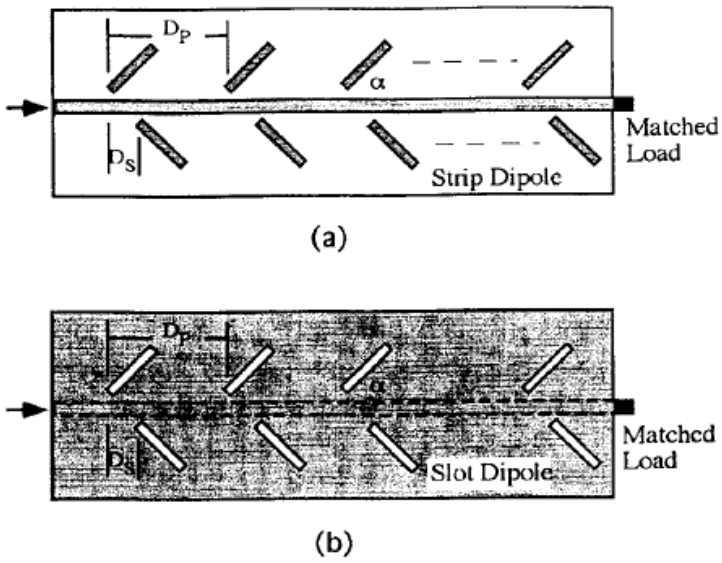

Figure 3.13 Traveling-Wave printed arrays for circular polarization: (a) dipole array and (b) slot array.

Other designs of traveling-wave arrays utilize a radiating propety at discontinuities the are periodicallyindroduced in traveling-wave transmission lines. In these designs , CP radiating element in each unit cell of the arrays is constructed from bending a microstrip feed line into an appropriate meander. Different design configurations reported in literature include rampart line antennas ,chain antennas, square-loop-type microstrip line antennas ,and creank-type microstrip line antenna. These configurations are shown in figure 3.14.

The rampart line antenna consists of four rectangular bends in each unit cell. The crank-type microstrip line antenna is simply two parallel rampart lines of the same dimensions with one line shifted by half a period. This arrangement results in better frequency characteristics for the axial ratio and radiation patern. For the chain antenna, its

fundamental element is built from a V-shape circularly polarized radiating element and a U-shape phase shifter while each unit cell of the square-loop . In the design , the period of the unit cell is less than λ_0 to avoid grating lobes, and the electrical line length in each unit cell should not be equal to a multiple of a guide wavelength to elliminate the situation in which small reflections can be combined in phase to produce a high return loss. These antennas radiate RHCP when they are fed from the left. The sense of the polarization is reversed when they are fed from right.

3.3 Singly Fed Circularly Polarized Microstrip Antennas (Rectangular-Type)

The following derivation is for different types of perturbations. They have been classified into type A and type B depending on the feed location. From figure 3.14 it is type A when the feed location is either on the x or y axis, where is in type B, the feed is placed on the diagonal axis of the patch. Note that the feed is always located diagonal to perturbation segments that are appropriately selected to produce two orthogonally degenerate modes in the patch for CP radiation.

The fundamental configuration of the patch and it's coordinate system are shown in figure 3.15. The square patch is considered to be an electrically thin cavity with perfect magnetic walls at the boundaries, x= ± a/2 and y= ± a/2. In the figure, F is the feed point and ΔS represents the total sum of the perturbation segments and may consists of single or multiple segments. The introduction of perturbation segments will affect the cavity model field and its eigen value, which can be determined from a stationary formula given by:

$$k'^2 = \frac{\int_{S+\Delta S} \nabla\phi' \cdot \nabla\phi' dS}{\int_{S+\Delta S} \phi'^2 dS} \qquad (3.1)$$

Where ϕ' and k' are the new model field and the new eigen value. ϕ' can be expanded as

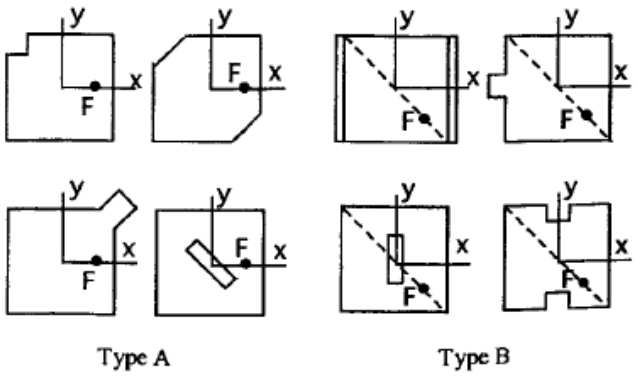

Figure 3.14 Various types of microstrip antenna perturbations for circular polarization generation

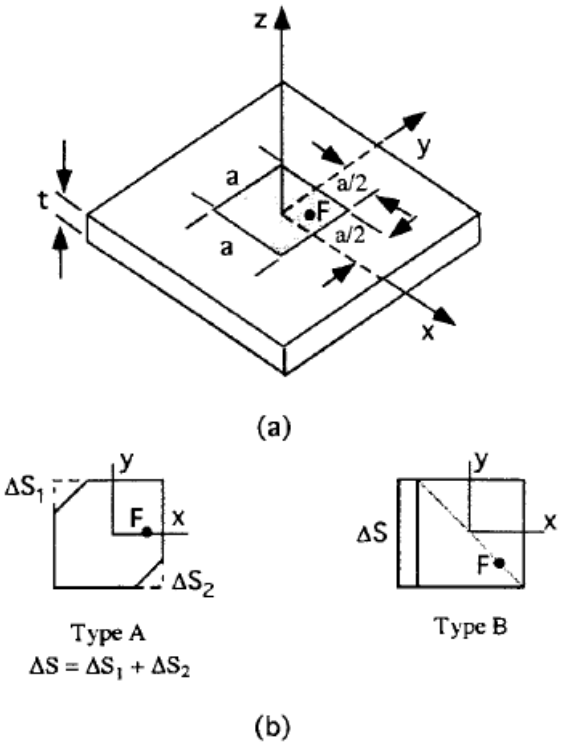

Figure 3.15 Configuration of singly fed microstrip patch antennas: (a) patch diagram and (b) type A and type B microstrip patch perturbations.

$$\phi' = P\phi_a + Q\phi_b \qquad (3.2)$$

Where P and Q are unknown expansion coefficients that have to be determined to make (3.1) stationary. Substituting (3.2) in (3.1) gives

$$k'^2 = \frac{\int_{S+\Delta S} (P\nabla\phi_a + Q\nabla\phi_b) \cdot (P\nabla\phi_a + Q\nabla\phi_b)\, dS}{\int_{S+\Delta S} (P\phi_a + Q\phi_b)^2 dS} = \frac{U(P, Q)}{V(P, Q)} \qquad (3.3)$$

Following the Ritz-Galerkin method, P and Q can be determined from

$$\begin{aligned} \frac{\partial U(P, Q)}{\partial P} - k'^2 \frac{\partial V(P, Q)}{\partial P} &= 0 \\ \frac{\partial U(P, Q)}{\partial Q} - k'^2 \frac{\partial V(P, Q)}{\partial Q} &= 0 \end{aligned} \qquad (3.4)$$

Equation (3.4) will result in a set of homogeneous equations that have nontrivial solutions only if the the determinant vanishes. Exact parameters of the determinant depend on the type of feed and perturbation placements. It can generally be written i the form

$$\det \begin{vmatrix} k^2 + q_1 - k'^2(1 + p_1) & q_{12} - k'^2 p_{12} \\ q_{12} - k'^2 p_{12} & k^2 + q_2 - k'^2(1 + p_1) \end{vmatrix} = 0 \qquad (3.5)$$

Type A Patch

For the type A-fed patch, ϕ_a and ϕ_b are the two normalized degerates modes, TM_{100} and TM_{010}, of a thin patch which can be written as

$$\begin{aligned} \phi_a &= V_0 \sin(kx) \\ \phi_b &= V_0 \sin(ky) \end{aligned} \qquad (3.6)$$

Where $k_0 = \sqrt{2}\frac{1}{a}$, $k = \frac{\pi}{a}$, and a is patch size. Using (3.6) in (3.2), all other parameters in (3.5) can be obtained from (3.4) as

$$\begin{aligned} q_1 &= q_2 = q_{12} = 0 \\ p_1 &= p_2 = 2\left(\frac{\Delta S}{S}\right) \\ p_{12} &= -2\left(\frac{\Delta S}{S}\right) \end{aligned} \qquad (3.7)$$

Substituting (8.7) into (8.5), the new eigen values k'_a and k'_b for the model fields ϕ_a and ϕ_b can be found from (8.5) as

$$\begin{aligned} k'^2_a &= k^2\left(1 + 4\frac{\Delta S}{S}\right)^{-1} \\ k'^2_b &= k^2 \end{aligned} \qquad (3.8)$$

From which the new resonant frequencies of ϕ'_a and ϕ'_b modes modes are obtained:

$$\begin{aligned} f_a &= f_{0r} + \Delta f'_a = f_{0r}\left(1 - 2\frac{\Delta S}{S}\right) \\ f_b &= f_{0r} + \Delta f'_b = f_{0r} \end{aligned} \qquad (3.9)$$

Where f_{0r} is the resonant frequency of the square patch before perturbation, and $\Delta f'_a$ and $\Delta f'_b$ are shifts in resonant frequencies for ϕ'_a and ϕ'_b modes after perturbation. Once the new eigen values k'_a and k'_b are determined, expansion coefficients P and Q can be found frrom the original set of homogeneous equations and are given by

$$\begin{aligned} P_a &= -Q_a = \frac{1}{\sqrt{2}} \\ P_b &= Q_b = \frac{1}{\sqrt{2}} \end{aligned} \qquad (3.10)$$

for the normalized ϕ'_a and ϕ'_b ,which can be written in slosed forms, using the first-order approximation of $k'_a \approx k'_b \approx k$, as

$$\phi'_a \approx \frac{V_0}{\sqrt{2}}(\sin(kx) - \sin(ky))$$
$$\phi'_b \approx \frac{V_0}{\sqrt{2}}(\sin(kx) + \sin(ky)) \qquad (3.11)$$

The energy distribution ratios for both ϕ'_a and ϕ'_b modes after perturbation are defined as turn ratios N'_a and N'_b, which are given by

$$N'_a = \frac{\sqrt{S}}{a}(\sin(kx) - \sin(ky))$$
$$N'_b = \frac{\sqrt{S}}{a}(\sin(kx) + \sin(ky)) \qquad (3.12)$$

Using (3.6)-(3.12), the equivalent circuit after perturbation can be derived as shown in figure 3.16. T'_A and T'_B represent ideal transformers with turn ratios N'_a and N'_b respectively, whereas V_f is input voltage applied to $1-1'$ terminal. $\dot{Y}_a$ and $\dot{Y}_b$ are the patch input admittances corresponding to the orthogonally polarized ϕ'_a and ϕ'_b modes.

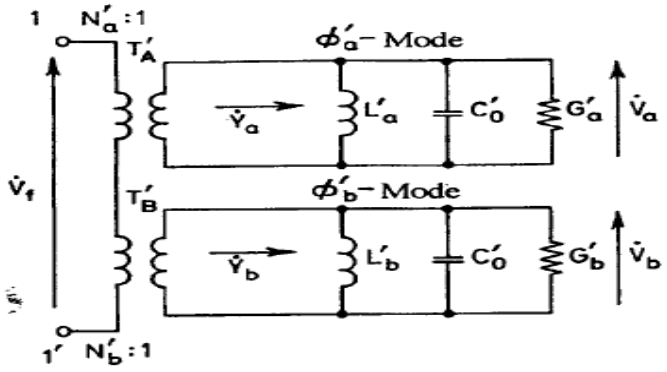

Figure 3.16 Equivalent circuit of microstrip patch antenna with perturbation.

The equivalent conductances G'_a and G'_b generally include radiation, dielectric, and copper losses. However, the radiation will be the main contribution to the conductances if it is dominant as compared with the other losses.

Type B patch

A similar procedure employed for type A can be applied to obtain different parameters for type B patch antenna, using the normalized modes ϕ_a and ϕ_b given by

$$\begin{aligned} \phi_a &= V_{00}(\sin(kx) + \sin(ky)) \\ \phi_b &= V_{00}(-\sin(kx) + \sin(ky)) \end{aligned} \qquad (3.13)$$

Where $V_{00} = 1/a$ and $k = \pi/a$. Other parameters are as follows:

$$p_1 = p_2 = \left(\frac{3}{2}\right)\left(\frac{\Delta S}{S}\right)$$

$$p_{12} = \left(-\frac{1}{2}\right)\left(\frac{\Delta S}{S}\right)$$

$$q_1 = q_2 = q_{12} = \left(\frac{1}{2}\right)\left(\frac{\Delta S}{S}\right)k^2$$

$$k_a'^2 = k^2\left(1 + 2\frac{\Delta S}{S}\right)^{-1}$$

$$k_b'^2 = k^2$$

$$f_a = f_{0r} + \Delta f'_a = f_{0r}\left(1 - \frac{\Delta S}{S}\right)$$

$$f_b = f_{0r} + \Delta f_b' = f_{0r}$$

$$\phi_a' = \left(\frac{\sqrt{2}}{a}\right)\left(1 - \frac{\Delta S}{S}\right)\sin(kx)$$

$$\phi_b' = \left(\frac{\sqrt{2}}{a}\right)\left(1 - \frac{\Delta S}{2S}\right)\sin(ky)$$

$$N_a' = \sqrt{S}\,\phi_a' \approx \sqrt{2}\sin(kx)$$

$$N_b' = \sqrt{S}\,\phi_b' \approx \sqrt{2}\sin(ky) \qquad \textbf{(3.14)}$$

The equivalent circuit in figure 3.17, the complex amplitude ratio V_z/V_b in the orthogonal modes is given by

$$\left(\frac{\dot{V}_b}{\dot{V}_a}\right) = \left(\frac{N_b'}{N_a'}\right)\left(\frac{Y_a'}{Y_b'}\right) = \left(\frac{N_b'}{N_a'}\right)\frac{\left\{\frac{f_a}{Q_0} + j\left(f - \frac{f_a^2}{f}\right)\right\}}{\left\{\frac{f_b}{Q_0} + j\left(f - \frac{f_b^2}{f}\right)\right\}} \qquad \textbf{(3.15)}$$

It is assumed in (3.15), to the first-order approximation, that the unloaded Q factors Q_{0a} and Q_{0b} of the two orthogonal modes ϕ_a' and ϕ_b' are equal to Q_0. For the patch to radiate CP, it is required that

$$\frac{Va}{Vb} = \pm j \qquad \textbf{(3.16)}$$

If the turn ratio N_a' and N_b' are selected such that

$$\frac{Nb'}{Na'} = \pm 1 \qquad \textbf{(3.17)}$$

Then (3.15) is reduced to

$$\left(\frac{\dot{V}_b}{\dot{V}_a}\right) = \pm \frac{\left\{\frac{f_a}{Q_0} + j\left(f - \frac{f_a^2}{f}\right)\right\}}{\left\{\frac{f_b}{Q_0} + j\left(f - \frac{f_b^2}{f}\right)\right\}} \qquad (3.18)$$

From (3.18), the frequency f and the perturbation segment ΔS/S can be determined in terms of Q_0 such that the CP radiation condition (3.16) is satisfied. This leads to the relation between ΔS/S and Q_0, which can be espressed as

$$\frac{(Q_0^2 - 1)Q_0^2}{(2Q_0^2 - 1)}(M^2 + N^2) = MN\left\{1 + \frac{(2Q_0^2 - 1)MN}{(M^2 + N^2)}\right\} \qquad (3.19)$$

Where M = (1+ mΔS/S), N = (1+nΔS/S), and m and n are the constants in $f_a = f_{0r}$ (1+ mΔS/S) and $f_b = f_{0r}$ (1+ nΔS/S), which are determined from the statinary formula as previously described.

Design Procedure for CP Patch With a Single-Point Feed

The general design procedure can be summarized as follows:

1. Determine the ubloaded Q_0 of the patch, which depends on dimensions a, substrate thickness t, and the substrate dielectric constant ε_r. For better accuracy Q_0 should be selected to ensure the patch radiation efficiency $\eta >$ 90%.
2. Determine the amount of perturbation (ΔS/S) for the type A and type B as follows:

   For type A

$$\left|\frac{\Delta S}{S}\right| = \frac{1}{2Q_0}$$

For type B

$$\left|\frac{\Delta S}{S}\right| = \frac{1}{Q_0}$$

3. The location of the feed point on the axis can be selected to provide a good match; alternatively a quarte-wavelength transformer can be used for matching purpose.
4. Depending on whether each type of the antenna is type A or type B, the sense of CP can be changed by switching the feed axis.

As s design example, a singly fed patch with dimension a = 9.14 mm on the substrate with thickness t = 1.18 mm and ε_r = 2.55 is demostrated for both type A and type B perturbations. First, the unloaded Q_0 and the radiation efficiency η vs substrate thickness t are plotted in figure 3.18. The value of Q_0 at t = 1.18 mm is found from the graph to be 28, which corresponds to the efficiency η exceeding 90%. At Q_0 = 28, the percentage of perturbation segment (ΔS/S) can be found from figure (3.17). For type A, ΔS/S is 2.9% and it is 6.5% for type B.

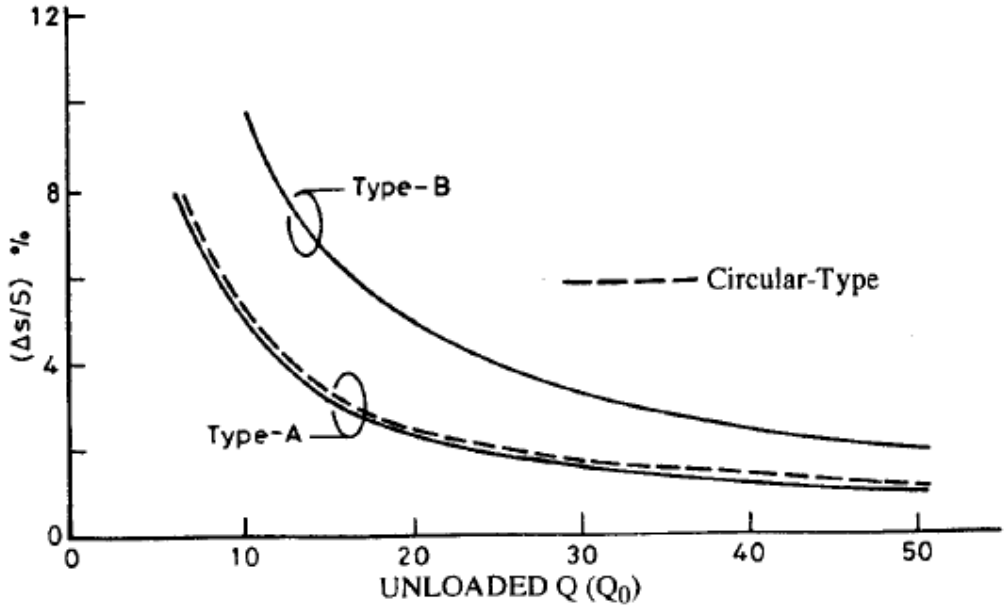

Figure 3.17 Variation of perturbation segments (ΔS/S) vs patch unloaded Q.

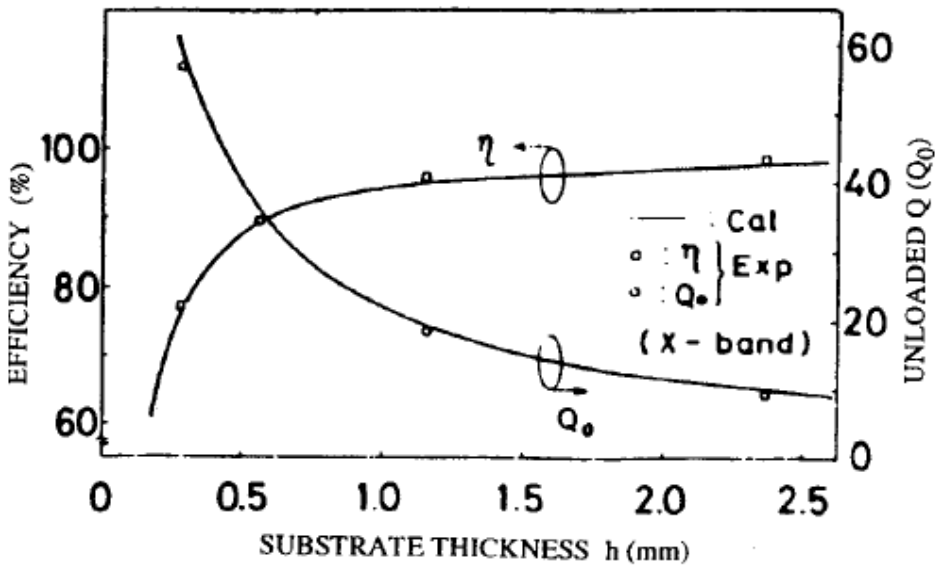

Figure 3.18 Variation of radiation efficiency η vs substrate thickness

3.4 Dual-Orthogonal Feed Circularly Polarized Microstrip Antennas

Use of a dual-feed technique is the most direct way to generate CP radiation from a square patch. The two orthogonal modes required for the generation of CP can be simultaneously excited using dual-orthogonal feeds. In designing, a patch is first matched to the feed lines by either appropriately selecting the feed locations or through the use of impedance transformers. The two feeds are then connected to the output ports of a power divider circuit, which provides the required amplitude and phase excitations. Various types of power divider circuits that have been successfully employed in a feed network of a CP patch are discussed in this section.

3.4.1 The Quadrature Hybrid

Referring to figure 3.19(a), the quadrature hybrid is a four-port network. Typically, the input is at port 1 and the output ports 2 and 3, while port 4 is terminated in a match load. Alternatively, port 4 can be the input and port 1match –terminated while the output remains at ports 2 and 3. With a high degree of symmetry, the operation of the hybrid is not affected when ports 1 and 4 are interchanged with ports 2 and 3. The basic

properties of the quadrature hybrid can be deduced directly from the scattering matrix, which is given by:

$$[S] = \frac{-1}{\sqrt{2}}\begin{bmatrix} 0 & j & 1 & 0 \\ j & 0 & 0 & 1 \\ 1 & 0 & 0 & j \\ 0 & 1 & j & 0 \end{bmatrix} \qquad (3.20)$$

As a power divider in a CP patch feed network, the input is connected to port 1 and 4 is match-terminated or vice versa,depending on the required sense of CP rotation. The output from ports 2 and 3 is then fed to the patch. The signal is evenly divided in amplitude but in phase quadrature at ports 2 and 3. Mismatch at the patch will return to the absorbing load at ports 4, thus a good match is maintained. Because ports 2 and 3 are uncoupled, good isolate ,generally exceeding 20 dB, also exists between the outputs. Consquently , the axial is not degraded.

A 3-dB quadrature hybrid can be designed using the expressions of a four-port direct-coupled power divider. The characteristic impedances Z_a and Z_b of a quarter-guide wavelength shunt and series arms are obtained as

$$Zb = \frac{Z0}{\sqrt{2}}$$

$$Za = Z0 \qquad (3.21)$$

3.4.2 The 180-Degree Hybrid

The ring hybrid, or a rat-race, is a 180-degree hybrid junction, as shown in figure 8.19(b). It is four-port network with the scattering matrix for the ideal 3-dB case given by

$$[S] = \frac{-j}{\sqrt{2}}\begin{bmatrix} 0 & 1 & 1 & 0 \\ 1 & 0 & 0 & -1 \\ 1 & 0 & 0 & 1 \\ 0 & -1 & 1 & 0 \end{bmatrix} \qquad (3.22)$$

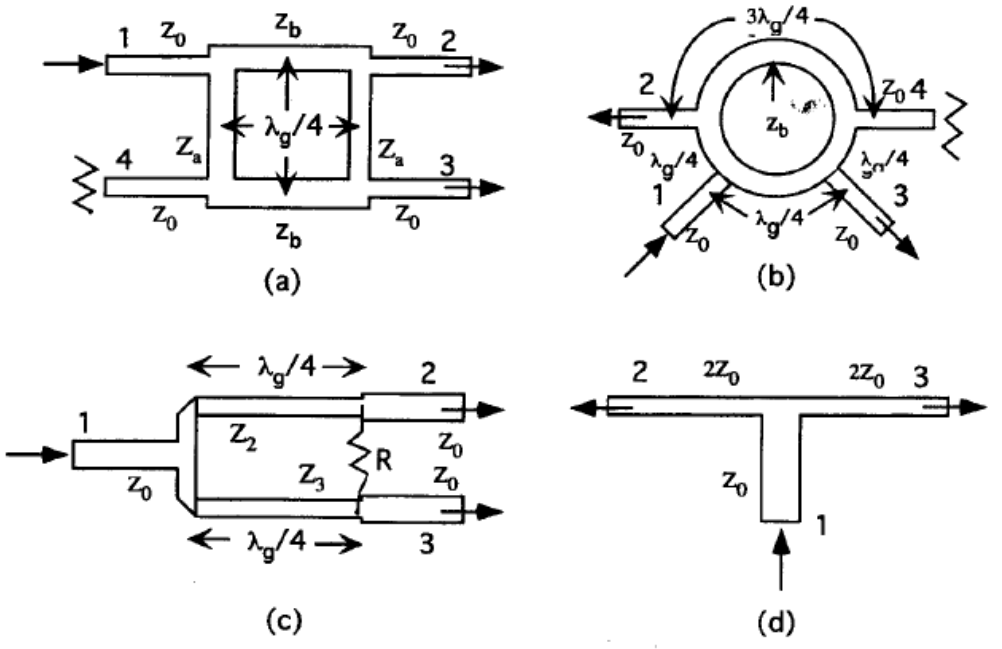

Figure 3.19 Schematic diagrams of power dividers (a) Quadrature Hybrid, (b) ring hybrid, (c) Wilkinson power divider, (d) T-Junction power divider.

The input at port 1 is equally split in amplitude and phase at the output ports 2 and 3, which are connected to the patch dual-orthogonal feeds. A quadrature phase different between the two orthogonal excitations can be achieved by a quadrature-wavelength differential line length between the two output lined. Because of the 90^0 phase shift between the output arms, any reflections from the patch tend to cancel at the output port 1 so that the match remains accepted. However, the combined mismatch at port 4 should be absorbed by a matched load to prevent potential power division degradation of the hybrid which, otherwise, can affect axial ratio performance. Because ports 2 and 3 are uncoupled, the isolation between the outputs is good. It is usually better than 20dB. When ports 4 becomes the input and port 1 is match-terminated while keeping everything else the same, the sense of CP rotation is changed.

The line parameters can be obtained from the general design equations of a hybrid-ring coupler. The characteristic impedance of the ring Z_b is found to be $\sqrt{2}Z_0$ for a 3-dB split.

3.4.3 The Wilkinson Power Divider

The Wilkinson power divider is generally an N- way hybrid splitter with arbitrary power division. In a CP feed network application, a Wilkinson will be considered to be a three-port device with the scattering matrix for the ideal case given by

$$[S] = \frac{-j}{\sqrt{2}}\begin{bmatrix} 0 & 1 & 1 \\ 1 & 0 & 0 \\ 1 & 0 & 0 \end{bmatrix} \qquad (3.23)$$

As depicted in figure 3.19(c), the input at port 1 is evenly divided in amplitude and phase at output ports 2 and 3. Similar to the ring hybrid previously described, at 90^0 phase difference at the dual feeds can be realized by a quarter-wavelength differential line length between the output arms of ports 2 and 3. As a result of a 90^0 phase shift between the two output arms, any reflection at the patch appears as odd mode excitation, which is dissipated in the isolation resistor. Hence, a good match is maintained, but the antenna efficiency may decrease. Good isolation between output ports 2 and 3 also prevents axial ratio degradation by the patch mismatch.

The line parameters for an equal-split Wilkinson power divider can be determined from design equations of the split-T power divider. They are given by

$$Z_2 = Z_3 = \sqrt{2}Z_0 \qquad (3.24)$$

$$R=2Z_0$$

3.4.4 The T-Junction Power Divider

The T-junction power divider as shown in figure 3.19(d) behaves similarly to a three-port Wilkinson except there is no isolation between output ports 2 and 3. Hence, the axial ratio is adversely affected by reflections tend to cancel each other at the input due to a quarter-wavelength difference between the two output arms. For equal split, the characteristic impedances in the T arms are given by $Z_2 = Z_3 = 2Z_0$.

General characteristics of these hybrids are summarized in Table 3.1

Table 3.1
General Characteristics of Power Divider Networks

	90° Phase Shift	Output Port Isolation	Input Match	Change of CP
T-junction divider	No*	No	Yes†	No
Wilkinson divider	No*	Yes	Yes†	No
Quadrature hybrid	Yes	Yes	Yes	Yes, by switching input and isolate ports
Ring hybrid	No*	Yes	Yes†	Yes,† by switching input and isolate ports

*Requires a quarter-wavelength of line extension in one output arm to generate phase shift.
†With a quarter-wavelength of line extension in one output arm in place.

Because a 3-dB quadrature hybrid produces fields with equal amplitudes and 90^0 phase without the need for a quarter-wavelength line extension in one of the feed arms, this results in a broader VSWR and axial ratio bandwidth as compared to other types of splitters.

3.4.5 Design Procedure

The design procedure for a dual orthogonal feed CP patch antenna can be summarized as follows:

1. Design a patch using two orthogonal feeds. Depending on applications, various types of feeding techniques can be employed, including direct contact methods such as probe or microstrip line feed and noncontacting feeds of proximity and slot couplings. Matching can be achieved by appropriately choosing the feed location and dimensions or by using impedance transformers.
2. A power divider network is selected and designed. The output ports are connected to antenna feeds. Impedance transformers can be used if necessary.

In design, it is preferable to minimize the coupling between the two feeds for a better axial ratio performance. If the coupling between the two feeds remains strong, a splitter with good isolation such as the quadrature hybrid or the Wilkinson divider is required for good quality.

Chapter 4

Microstrip Patch Antenna Design and Results

4.1 Introduction

In this chapter, the procedure for designing a square microstrip patch antenna in IE3D software is explained. And the results obtained from the simulations are demonstrated.

4.2 Design Specifications

The three essential parameters for the design of a rectangular Microstrip Patch Antenna are:

- Frequency of operation (f_o): The resonant frequency of the antenna must be selected appropriately. The Mobile Communication Systems uses the frequency range from 1800-5600 MHz. Hence the antenna designed must be able to operate in this frequency range. The resonant frequency selected for my design is 3.0 GHz.

- Dielectric constant of the substrate (ε_r): The dielectric material selected for my design is silicon which has a dielectric constant of 2.55. A substrate with a high dielectric constant has been selected since it reduces the dimensions of the antenna.

- Height of dielectric substrate (h): For the microstrip patch antenna to be used in cellular phones, it is essential that the antenna is not bulky. Hence, the height of the dielectric substrate is selected as 1.59 mm.

Hence, the essential parameters for the design are:

- f_o = 3.0 GHz
- ε_r = 2.55
- h = 1.59 mm

4.3 Design of Square Patch Microstrip Antenna for Circular Polarization using IE3D Simulator

Given specifications were,

1. Dielectric constant (ε_r) = 2.55
2. Frequency (f_r) = 3.0 GHz.
3. Height (h) = 1/16 Inch = 1.59 mm.
4. Velocity of light (c) = 3×10^8 ms^{-1} .
5. Practical width (W) , W = 30 mm.
6. Loss Tangent (tan δ) = 0.001.
7. Practical Length (L) L = 30 mm.

4.3.1 Simulation in IE3D

1. Start Zeland Program Manager.

2. Double click on mgrid.

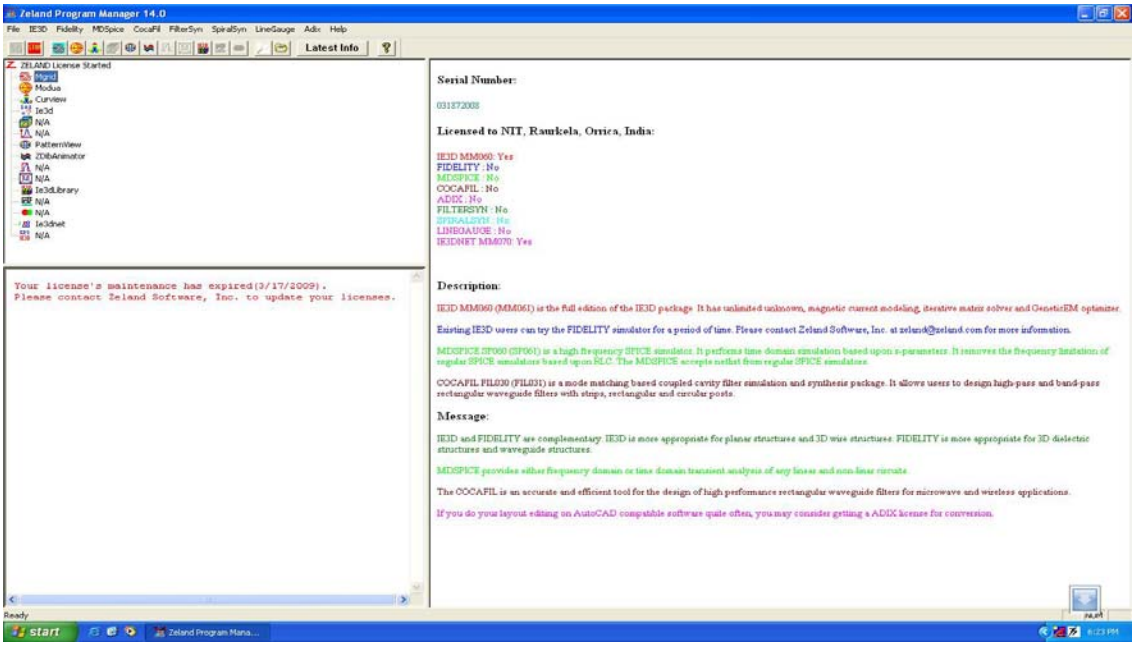

3. Click on File →Open New File.

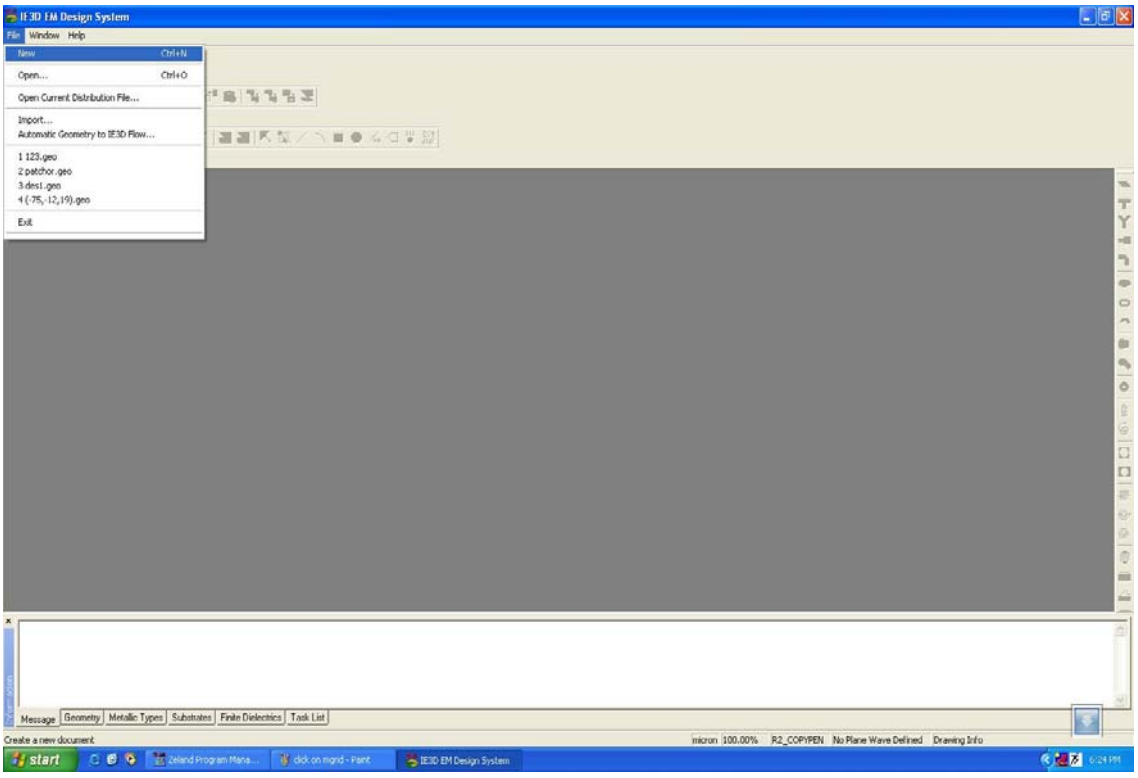

4. Make Grid Size 0.025 mm.

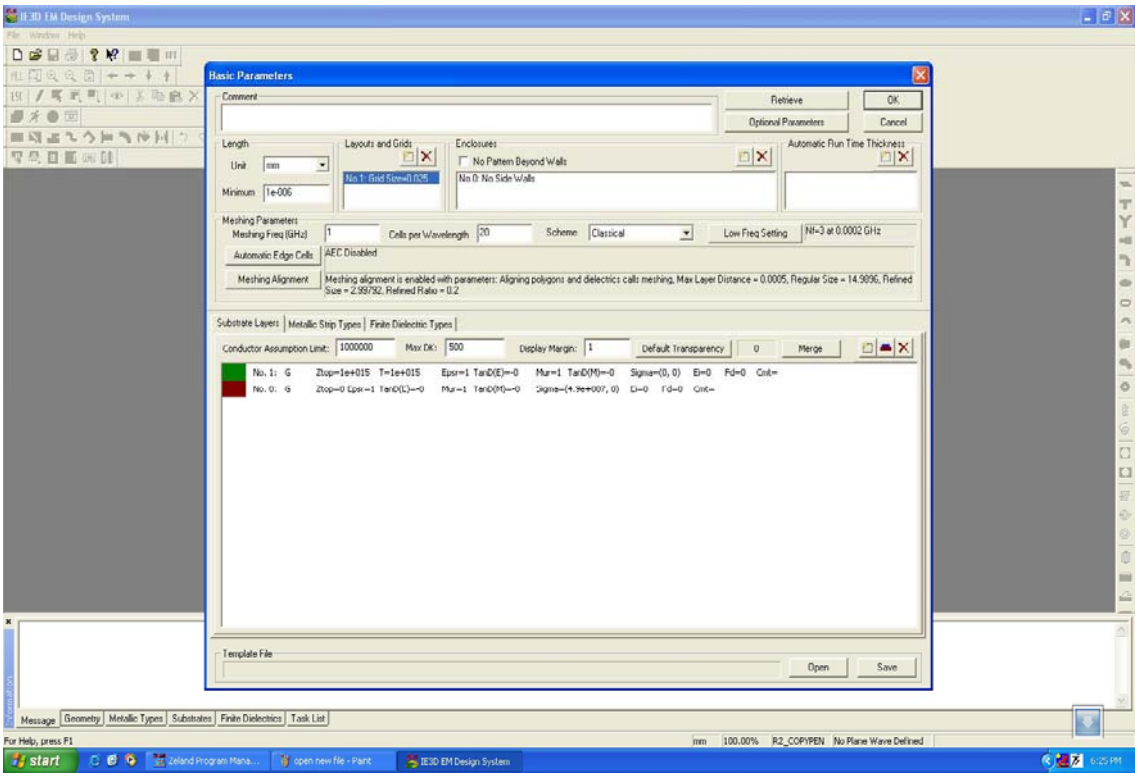

5. Define Substrate Parameters

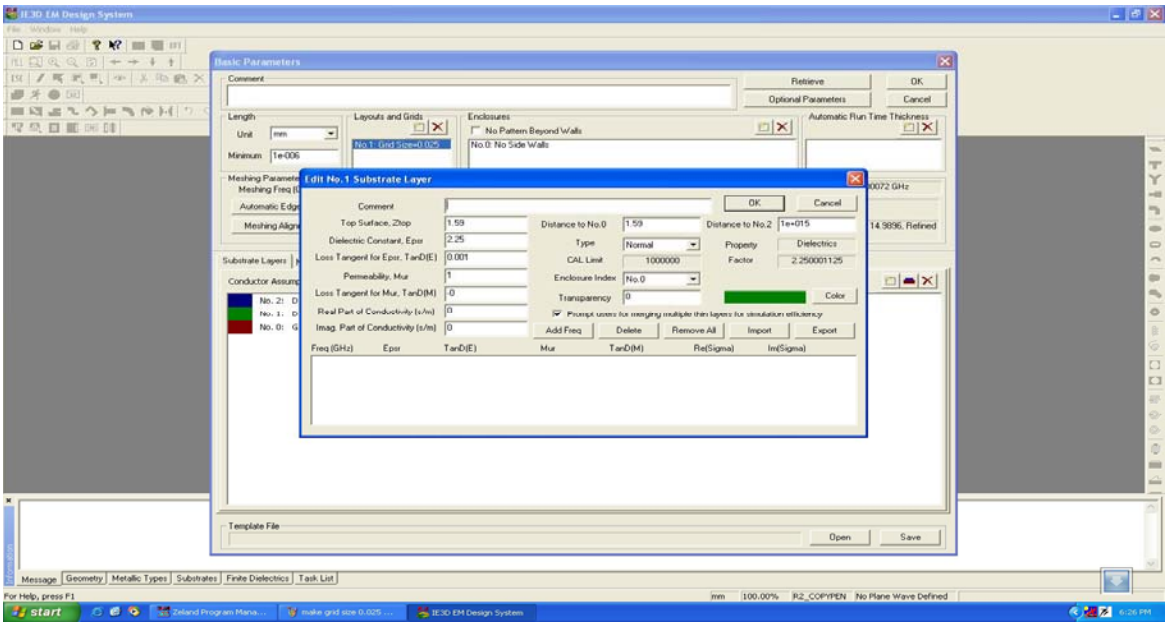

6. Click on Entity → Rectangle

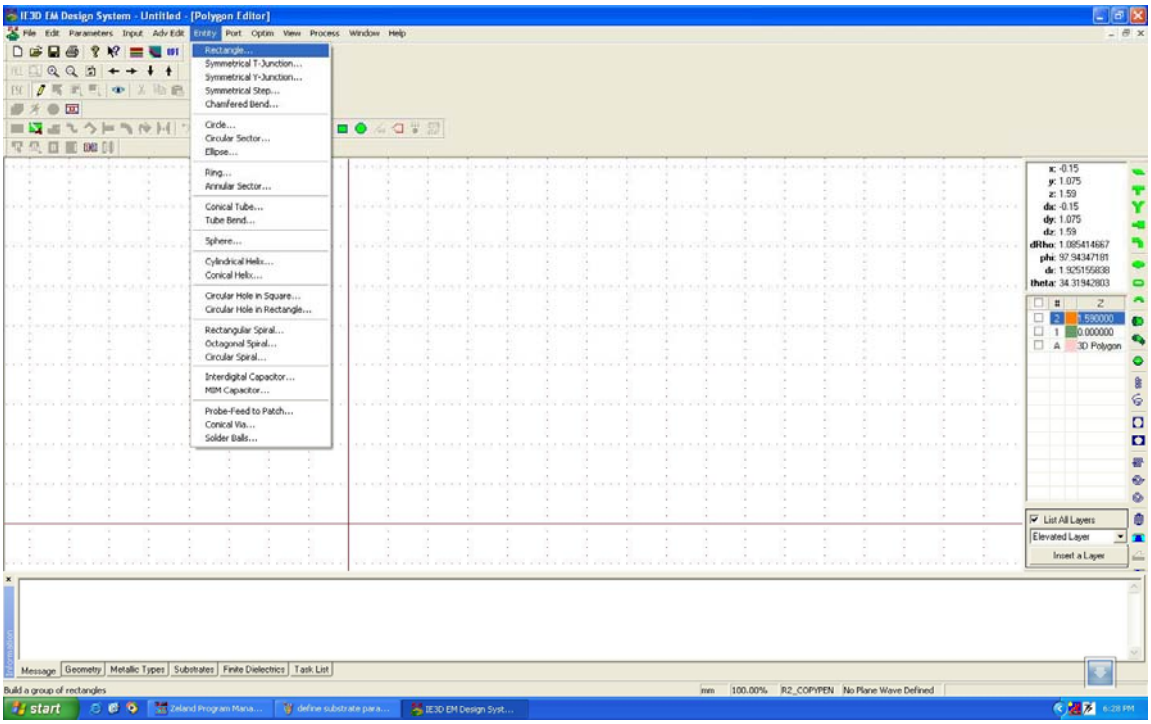

7. Click on Entity → Probe Feed to Patch

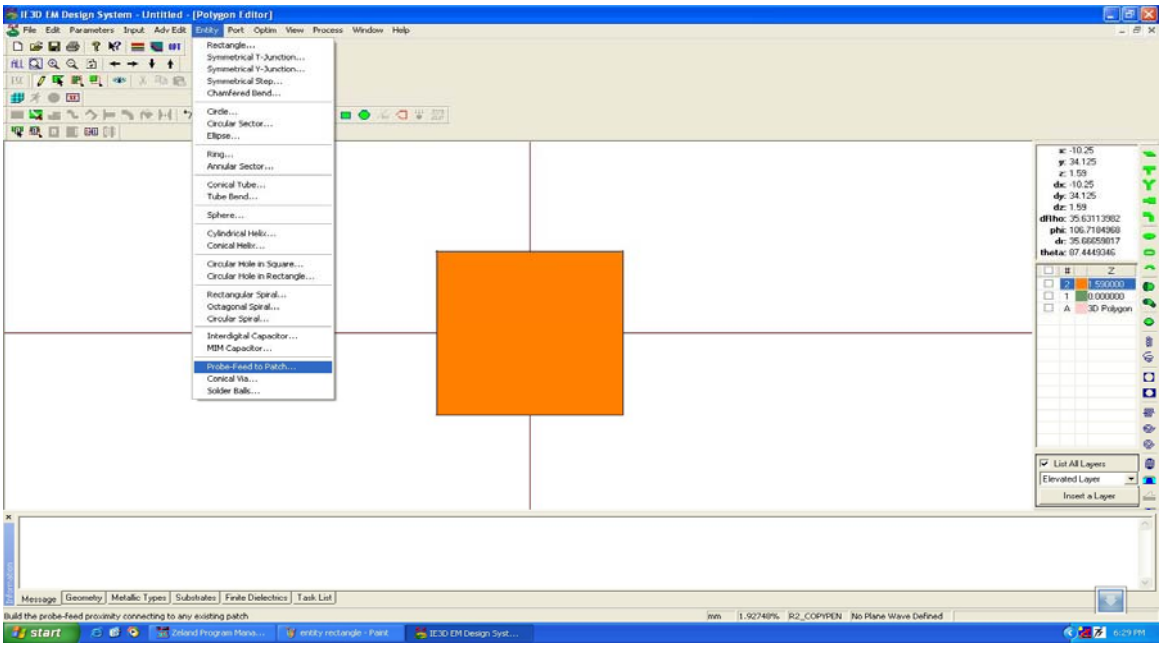

8. Give Location of first Feed Point

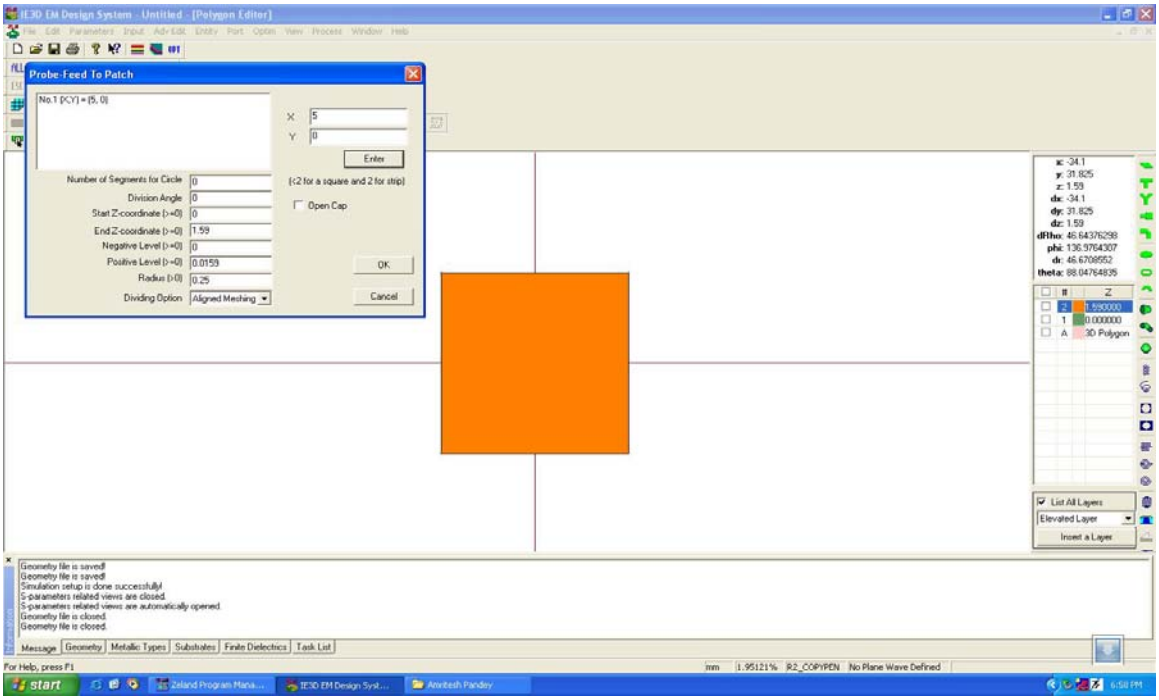

9. Give Location to Second Feed Point.

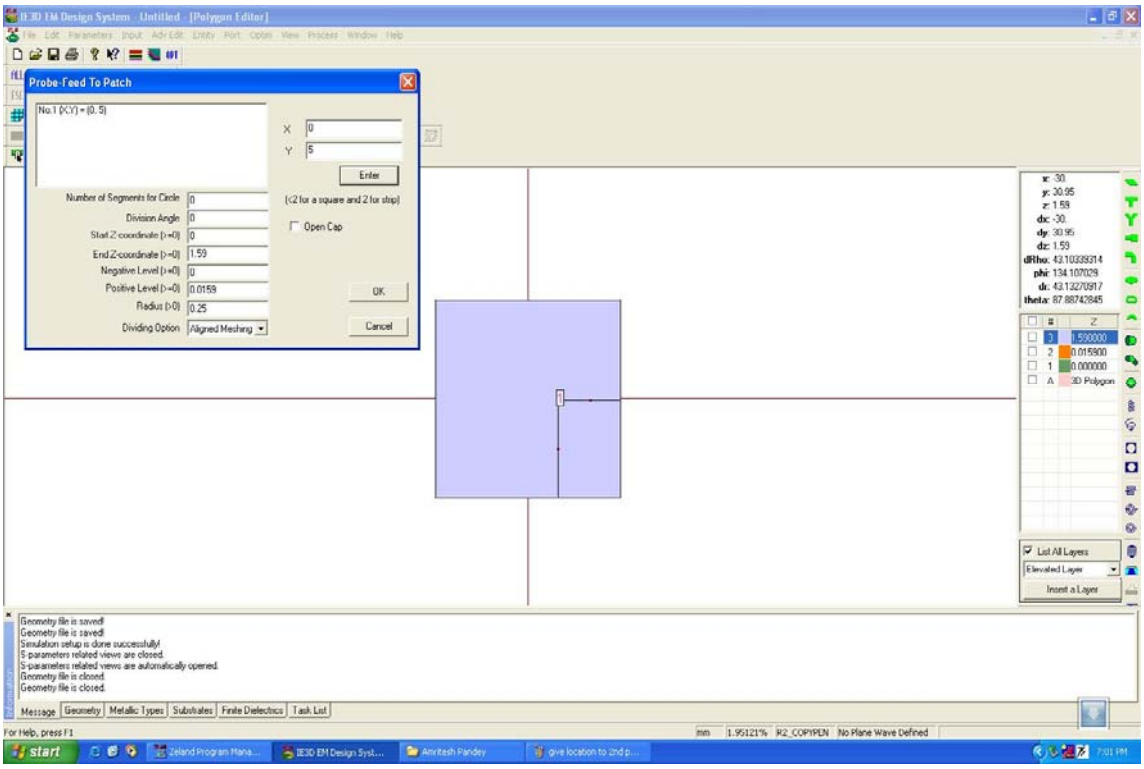

10. Go to Adv Edit → Rectanglization

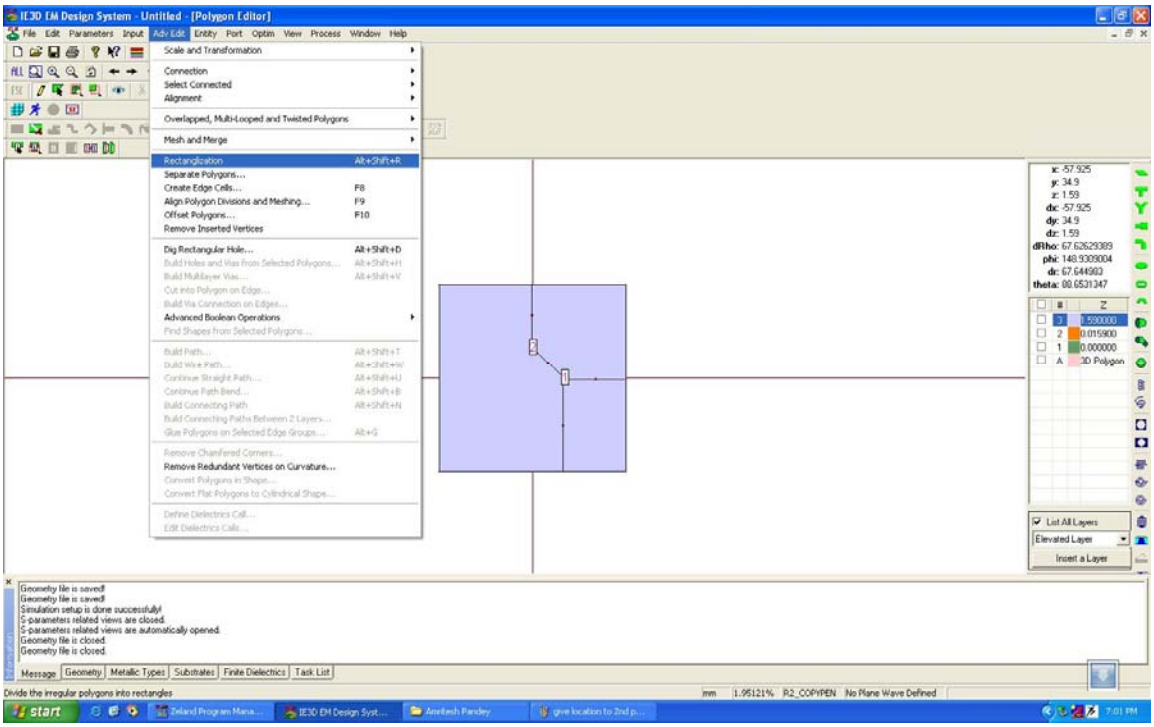

11. Click on Process → Simulate

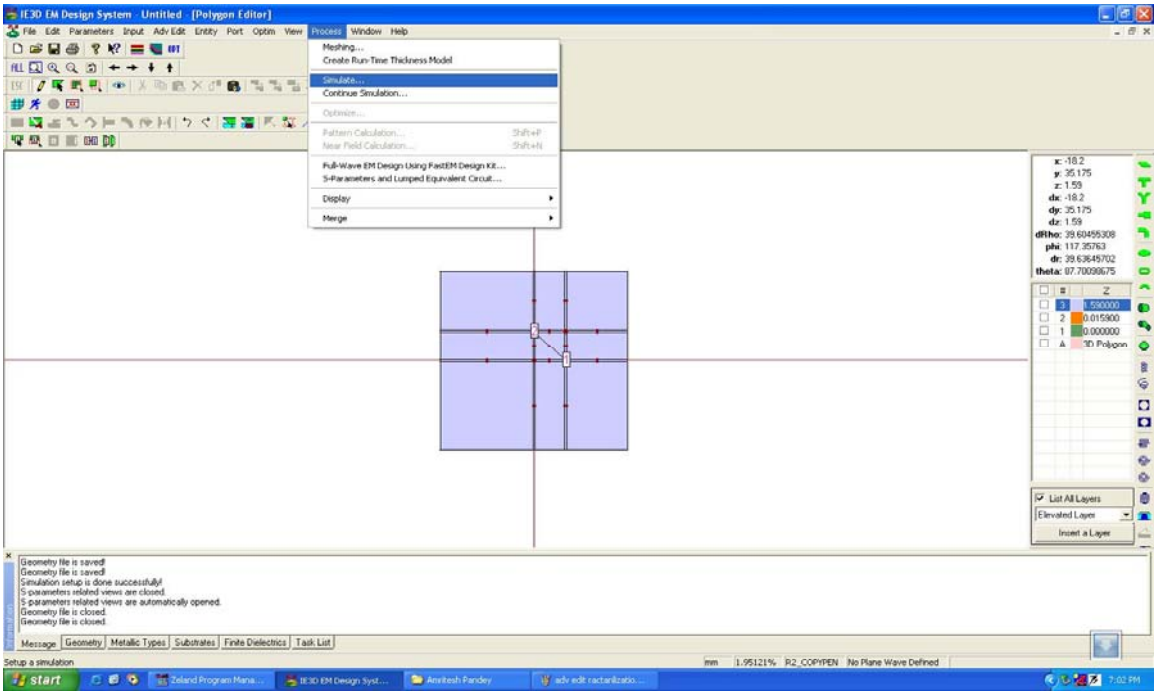

12. Enter Frequencies

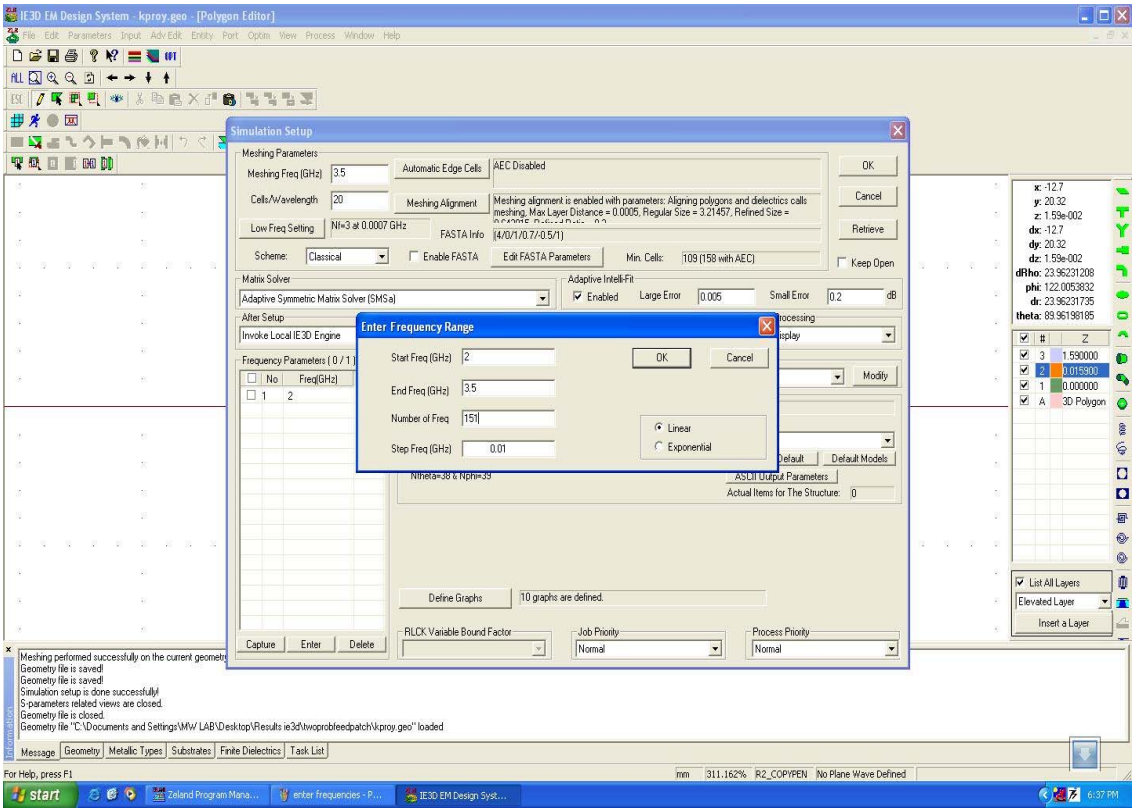

13. Press OK.
14. Simulation Starts and after simulation we get the results.

4.3.2 Results of Simulation

DesignedPatch

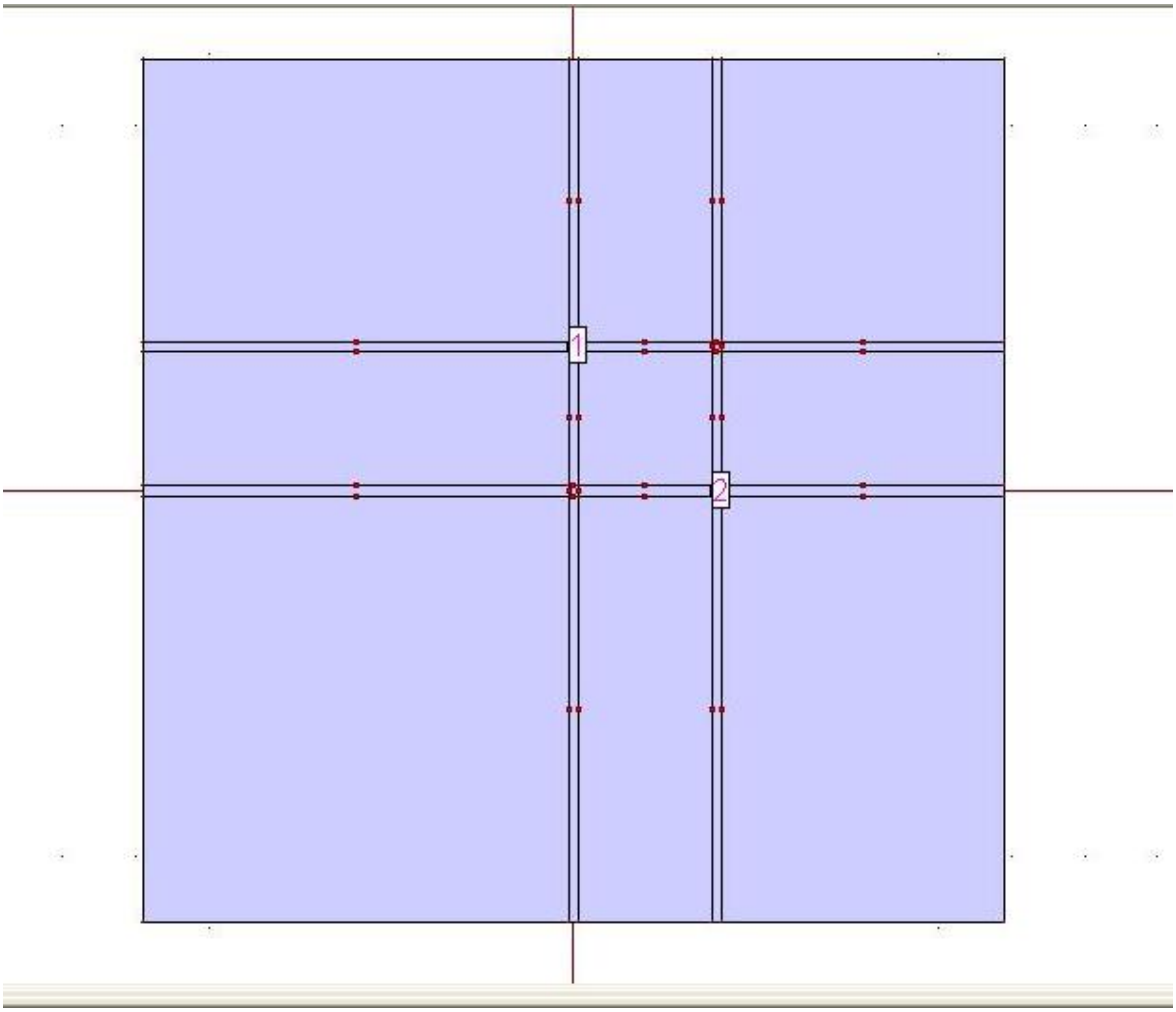

Figure 4.1 Patch Designed in IE3D Software

S-Parameters

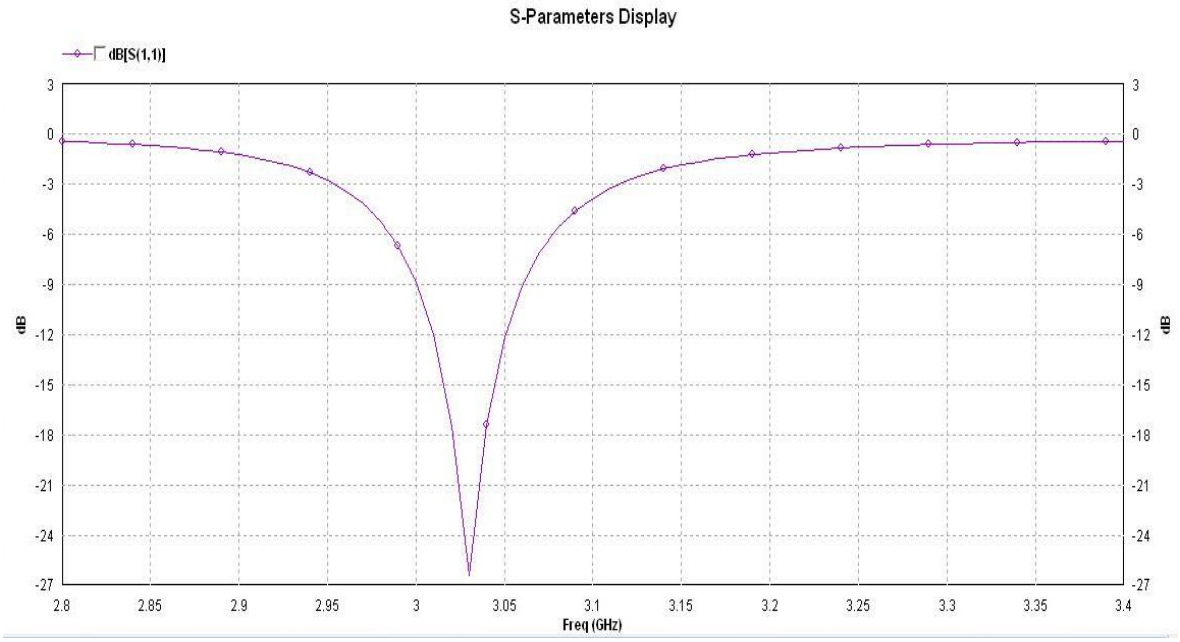

Figure 4.2 S-Parameter Display for S(1,1)

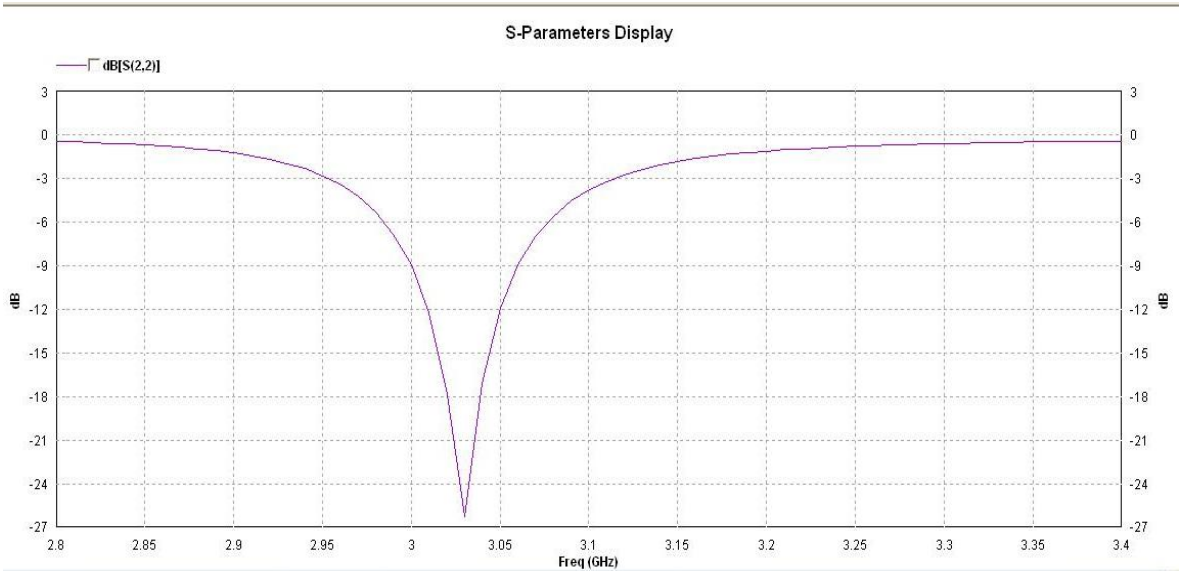

Figure 4.3 S-Parameter Display for S(2,2)

Smith Charts

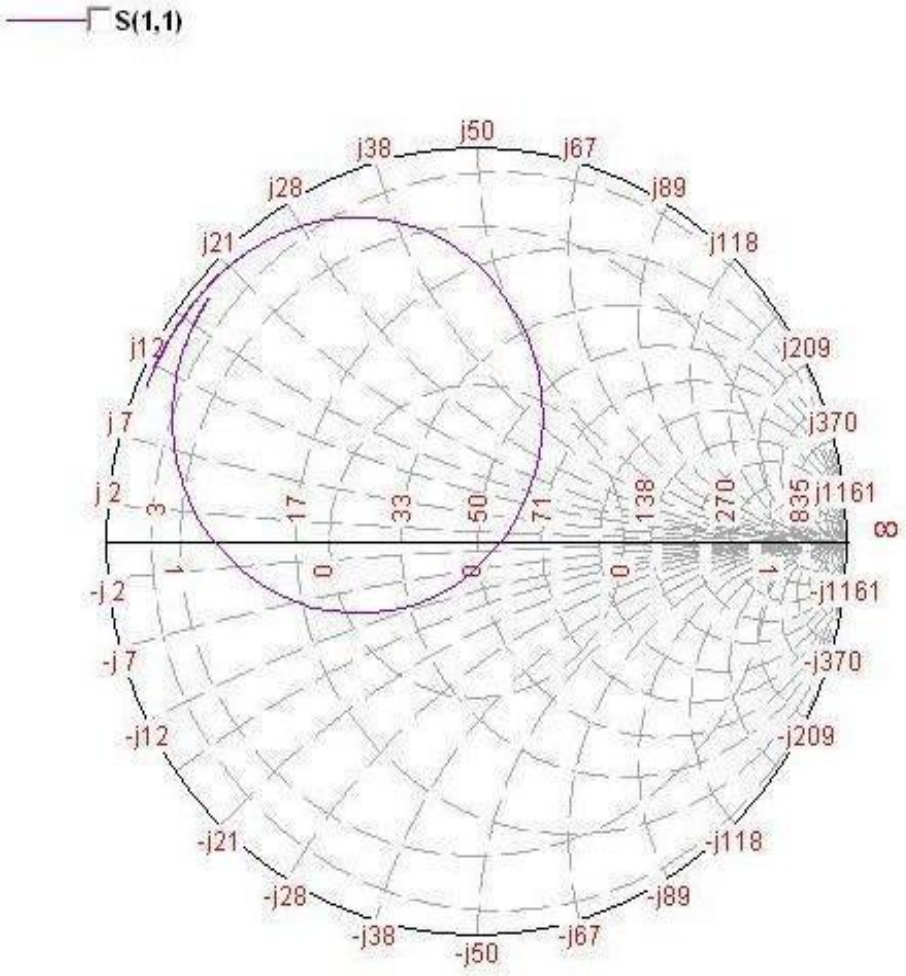

Figure 4.4 Smith Chart Display for S(1,1)

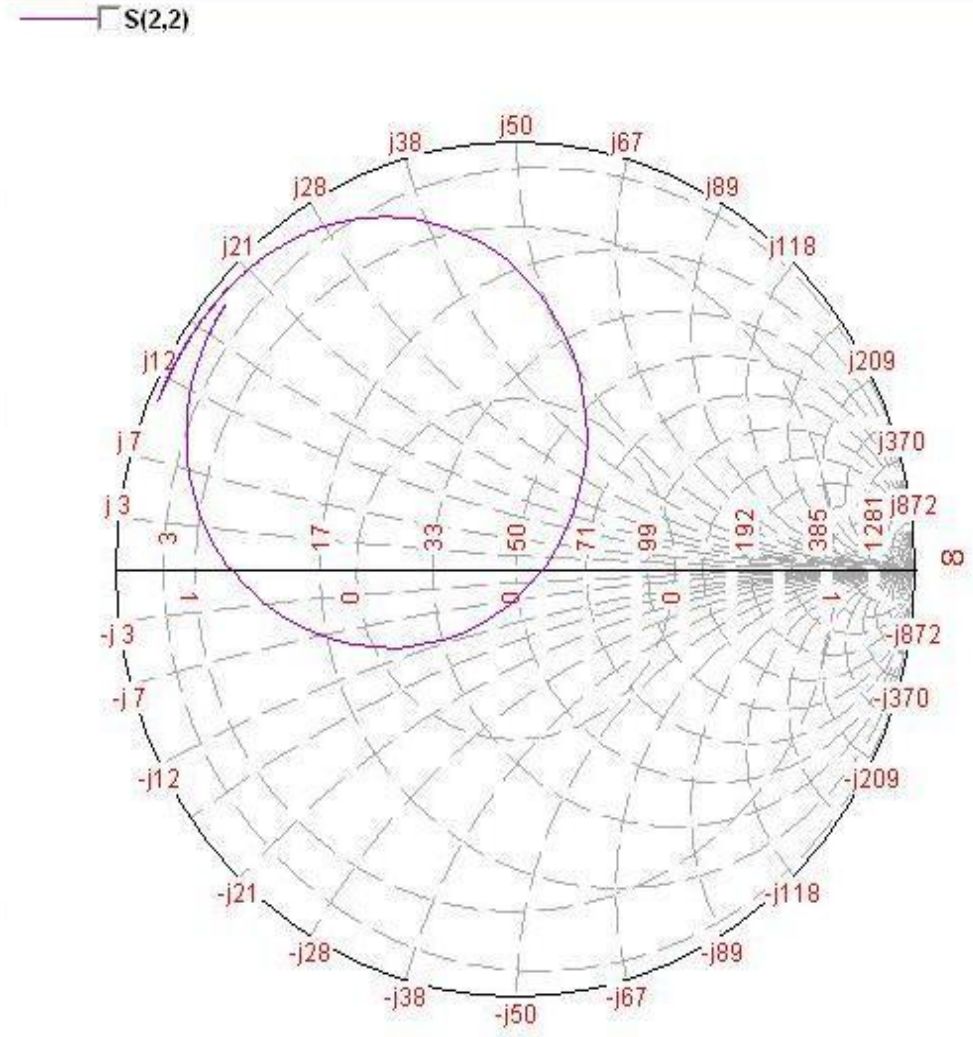

Figure 4.5 Smith Chart Display for S(2,2)

Voltage Standing Wave Ratio (VSWR)

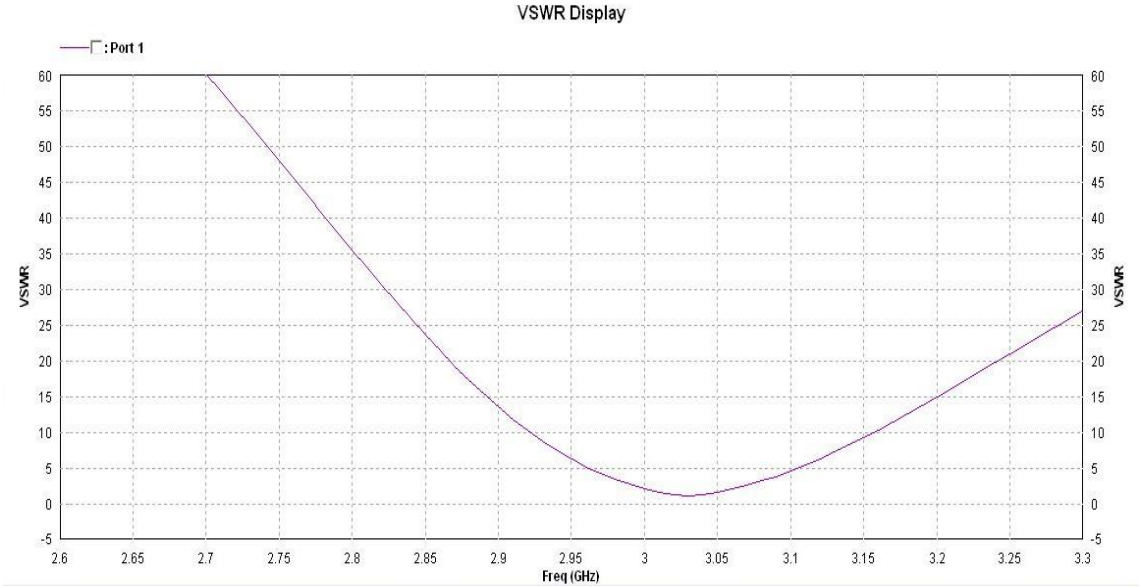

Figure 4.6 VSWR for Port 1

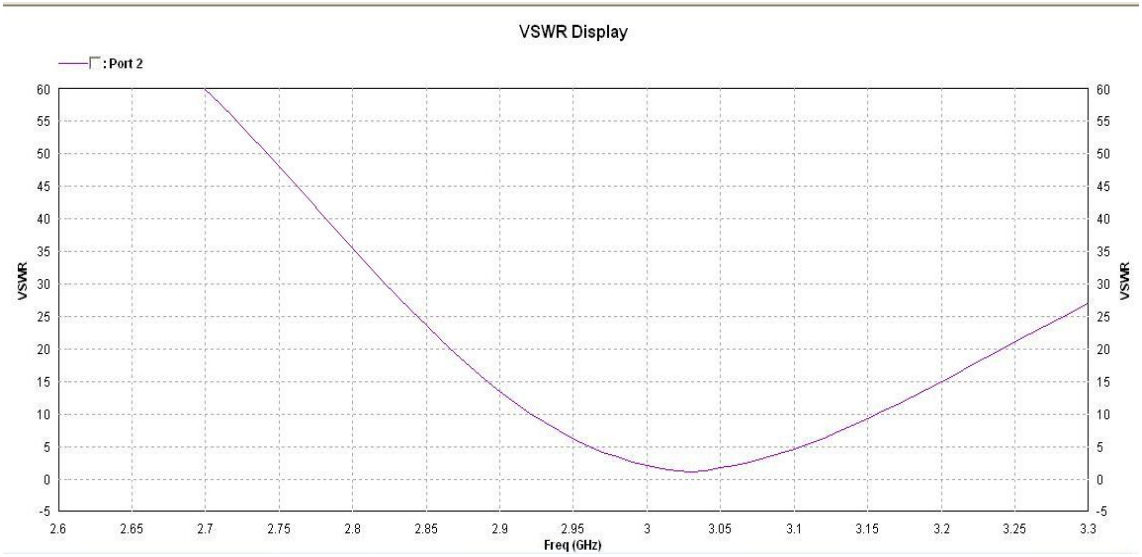

Figure 4.7 VSWR for Port 2

3D Current Distribution

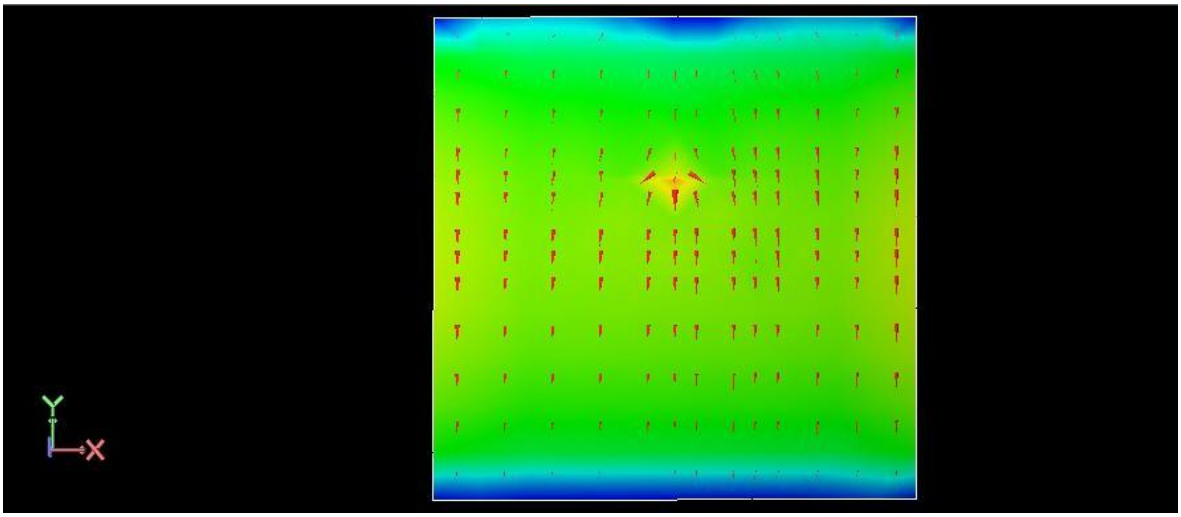

Figure 4.7 3D Current Distribution

Elevation Pattern Gain Display

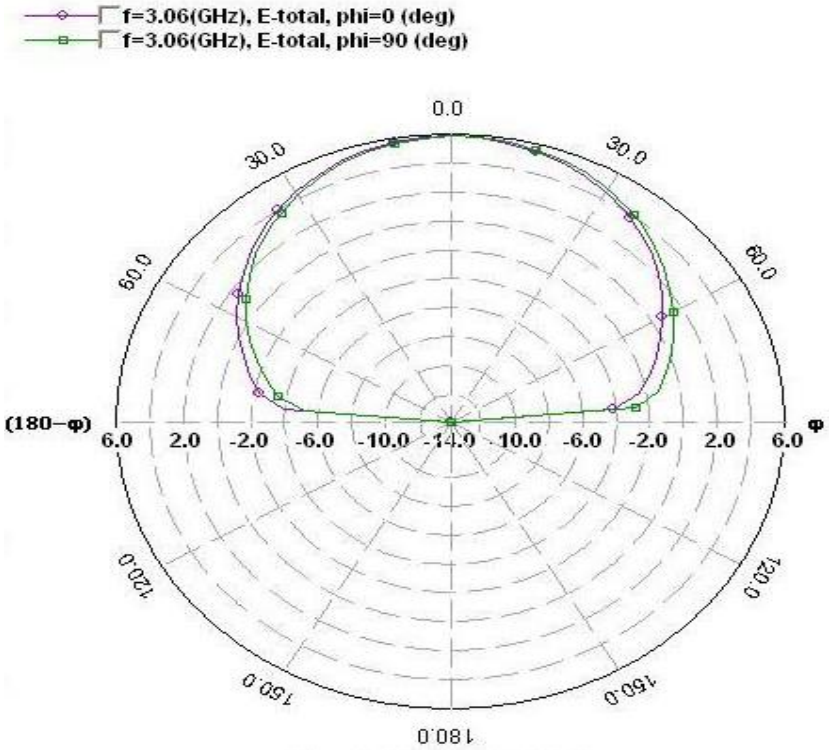

Figure 4.11 Elevation Pattern Gain Display (dBi)

Total Gain vs. Frequency Graph

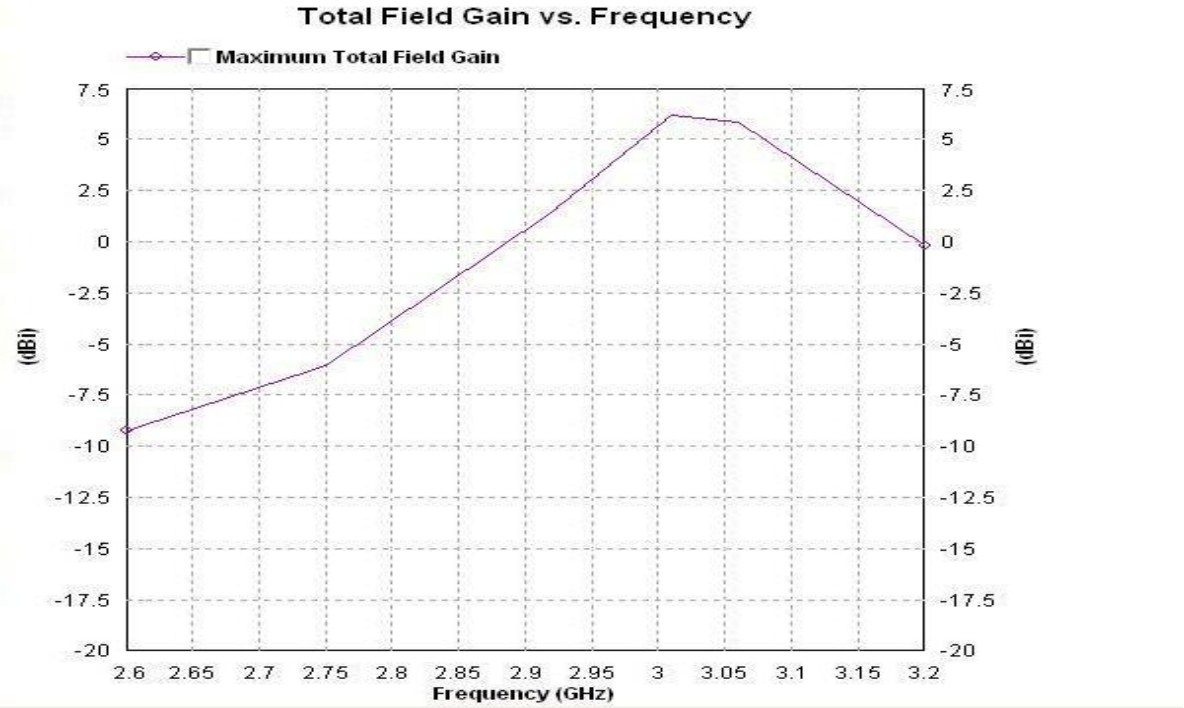

Figure 4.12 Gain vs Frequency

Axial Ratio vs. Frequency Graph

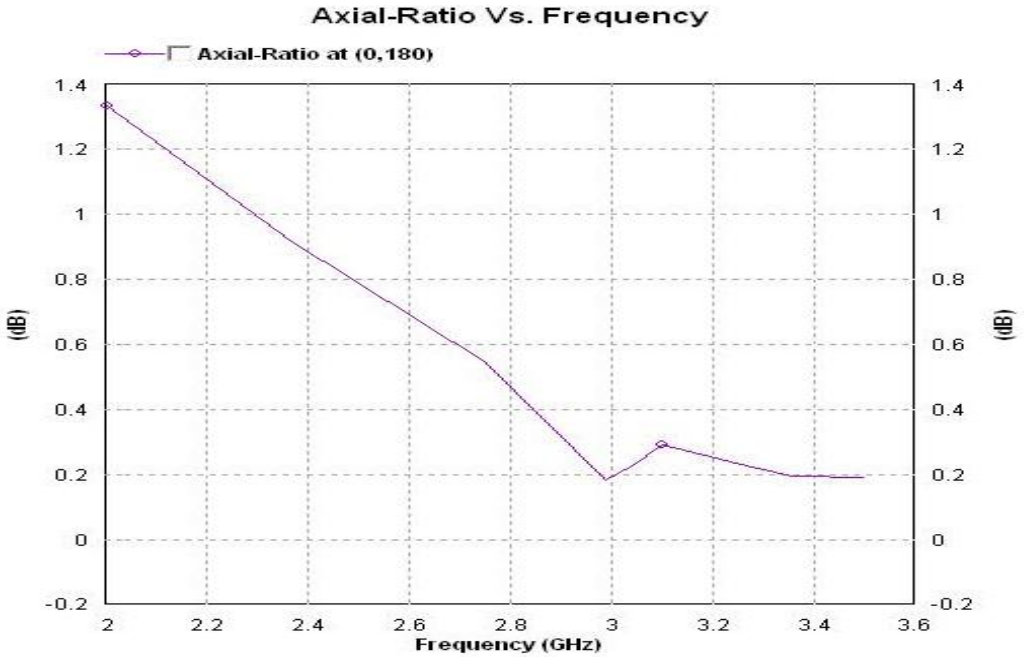

Figure 4.13 Axial Ratio vs. Frequency Plot

Chapter 5

Conclusion and Future Scope

The design of Square patch dual feed (Probe Feed) antenna for circular polarization has been completed using IE3D software. The simulation gave results good enough to satisfy our requirements to fabricate it on hardware which can be used wherever needed. The investigation has been limited mostly to theoretical studies and simulations due to lack of fabrication facilities. Detailed experimental studies can be taken up at a later stage to fabricate the antenna. Before going for fabrication we can optimize the parameters of antenna using one of the soft computing techniques known as Particle Swarm Optimization (PSO).

References:

[1] C. A. Balanis, " Antenna Theory, Analysis and Design", JOHN WILEY & SONS, INC, New York 1997.

[2] R. Garg, P. Bhartia, I. Bahl, A. Ittipiboon, "Microstrip Antenna Design Handbook", ARTECH HOUSE, Boston 2001.

[3] S. Silver, "Microwave Antenna Theory and Design", McGRAW-HILL BOOK COMPANY, INC, New York 1949.

[4] D. M. Pozar and D. H. Schaubert, Microstrip Antennas: The Analysis and Design of Microstrip Antennas and Arrays, IEEE Press, 1995.

[5] K. F. Lee, Ed., Advances in Microstrip and Printed Antennas, John Wiley, 1997.

[6] F. E. Gardiol, "Broadband Patch Antennas," Artech House.

[7] D. R. Jackson and J. T. Williams, "A comparison of CAD models for radiation from rectangular microstrip patches," Intl. Journal of Microwave and Millimeter-Wave Computer Aided Design, Vol. 1, No. 2, pp. 236-248, April 1991.

[8] D. R. Jackson, S. A. Long, J. T. Williams, and V. B. Davis, "Computer aided design of rectangular microstrip antennas", Ch. 5 of Advances in Microstrip and Printed Antennas, K. F. Lee, Editor, John Wiley, 1997.

[9] J.-F. Zürcher and F. E. Gardiol, Broadband Patch Antennas, Artech House, 1995.

[10] H. Pues and A Van de Capelle, "Accurate transmission-line model for the rectangular microstrip antenna," Proc. IEE, vol. 131, pt. H, no. 6, pp. 334-340, Dec. 1984.

[11] D. M. Pozar, "Input impedance and mutual coupling of rectangular microstrip antennas," IEEE Trans. Antennas and Propagation, vol. AP-30, pp. 1191-1196, Nov. 1982.

[12] C. J. Prior and P. S. Hall, "Microstrip disk antenna with short-circuited annular ring," Electronics Letters, Vol. 21, pp. 719-721, 1985.

[13] Y.-X. Guo, C-L. Mak, K-M Luk, and K.-F. Lee, "Analysis and design of Lprobe proximity fed patch antennas," IEEE Trans. Antennas and Propagation, Vol. AP-49, pp. 145-149, Feb. 2001.

[14] K. Ghorbani and R. B. Waterhouse, "Ultrabroadband printed (UBP) antenna," IEEE Trans. Antennas and Propagation, vol. AP-50, pp. 1697-1705, Dec. 2002.

[15] G. Kumar and K. C. Gupta, "Non-radiating edges and four edges gap coupled multiple resonator broadband microstrip antennas," IEEE Trans. Antennas and Propagation, vol. AP-33, pp. 173-178, Feb. 1985.